Characterization of State of Wear and available Friction by Inspection of 3D Surface Scans Generated by Laser Profilometry

Thesis

Presented in Partial Fulfillment of the Requirement for the Degree Bachelor of Science, Honors Research Distinction at The Ohio State University

By

Gage S. Sovey

College of Engineering, Mechanical Engineering

The Ohio State University

2020

Thesis Committee:

Rebecca B. Dupaix, Advisor

Jeffrey P. Chrstos

Abstract

As a road surface is traveled on, a polishing phenomenon occurs. Depending on the binder used, aggregate used, and period in the life cycle of the road this polishing can either improve or hurt friction performance of the surface. Being able to accurately predict change in friction as wear occurs changing the surface texture of a road is desirable. Due to this desire, the studies discussed in this thesis aim to correlate the surface changes associated with state of wear of a surface with the available friction provided by the surface to the tire. During experimentation two road samples (pills) prepared in the lab were polished and tested at 15-minute intervals for a total of two hours. After polishing, the pills were tested on the British Pendulum Tester and then scanned using a laser texture scanner. The scan data was then filtered and post processed to obtain the spectral data of the surface profile. The results of surface spectra and friction responses were then examined for correlations. Examination of different comparisons between polishing time, friction response, and road surface data was conducted to search for a relationship between wear and friction.

Acknowledgments

Firstly, I would like to thank Dr. Rebecca Dupaix and Dr. Jeffrey Chrstos for allowing me to be a part of this project. Throughout my time working on the team they have imparted on me a wealth of technical, professional, academic, and life advice. I am appreciative of this and hope I wasn't too much trouble.

Secondly, I would like to thank a handful of people who made this thesis possible. I would like to thank Ryan Walton, Ruban Sekar, and Joey Staschiak for their previous work which was essential to the life of this study. I would also like to thank the Highway Infrastructure Management Team at the Ohio Department of Transportation for helping with data collection and providing high expertise to the project.

Finally, I would like to thank my family for working hard to afford me a life full of opportunity, happiness, and love. I am eternally grateful for the sacrifices they have made for me and hope that I can live up to the high standard they have set.

Table of Contents

List of Tables

List of Figures

Chapter 1: Introduction

Motivation

This thesis aims to draw a link between the state of wear of a road surface and the available friction of that surface. This will be inspected by polishing road samples in the lab to study wear due to travel on a road surface. This kind of wear is one variable that goes into the total aging of a road surface.

There are two main pillars of motivation for this project. The first of these pillars is safety. Currently, the most accurate method of testing available road friction is the use of skid trucks. These trucks work by dragging a trailer outfitted with control and measurement equipment and suddenly locking up one of the wheels. Once the wheel is locked up the reaction forced experienced by the axle is measured and the ratio of longitudinal force developed by friction on the locked-up wheel to its normal force is calculated. This number is reported as the skid number and is widely used as a metric to assess available road friction and ultimately safety. These trucks cost hundreds of thousands of dollars and require specific testing conditions which are often hard to achieve on live roadways. A quick and inexpensive way to examine road condition would improve the ability of organizations such as the Department of Transportation to test more surfaces more rapidly. This would prevent unsafe roads from going undetected and for already thinly stretched resources to be more effectively allocated. Ultimately, this would help identify surfaces that need to be repaired more efficiently having a positive impact on traffic safety.

The second pillar is performance. Development of a quick method to assess road friction would allow companies such as tire and auto manufacturers to test in near real time the performance characteristics of their proving grounds. This would help them understand testing data obtained over different conditions and surfaces and improve their ability to fine tune product performance. A significant advantage on race day would also come as a byproduct of this technology. Being able to rapidly examine a track would allow teams to understand what strategies are the most advantageous in the present track conditions. This is extremely valuable in situations like the Daytona finish below in figure 1, where typical prize differences between first and second place are close to a half million dollars.

Figure 1: Close Finish at Daytona [5]

Background

Friction

Friction developed between standard passenger vehicle rubber tires and road surfaces is dominated by two mechanisms. These mechanisms are the energy losses associated with

hysteresis of the tire and adhesion losses resulting from momentary bonding between tire rubber and the road. [6]

Since tires are made of viscoelastic material, they deform into small imperfections on the road surface as they slide over them. Losses are then experienced as they retake their initial shape after the tire contact patch has rotated away due to not having a perfectly elastic nature.

Adhesion losses are due to the energy which is required to break intermolecular bonding occurring between the tire and road surface. Not much is known about this method of friction but phenomena such as “rubbering in” of racetracks suggests it is the dominating mechanism of friction development. [6]

Wet road conditions also affect the friction available to the tire. Since adhesion is negatively affected by the presence of water, adhesion is significantly reduced in wet conditions. Since this is the most significant contributor to performance, available friction is greatly reduced in wet road conditions. Wet roads also contribute to the phenomenon of hydroplaning. This is the condition where a film of water separates the tire from the road causing a loss in control over the vehicle. Since hysteresis is largely unaffected by wet conditions provided an absence of hydroplaning, high-hysteresis tires perform much better in wet surface scenarios. [6]

As the other half the other tire road interface, road surface characteristics also contribute largely to friction. Figure 2 below shows the regions of road surface texture.

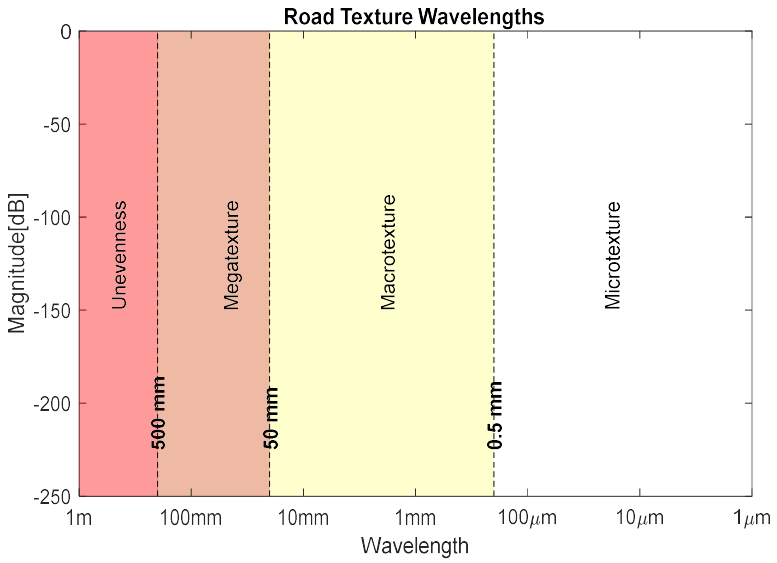

Figure 2: Road Texture Regions[3]

The two regions of concern relative to friction performance are micro texture and macrotexture. Microtexture is defined and the texture contributions with wavelengths between 1 micron and a half millimeter. This region of road texture is responsible for micro-hysteresis and adhesion. This region is the most compromised by the presence of water on the road surface. Macrotexture which is defined as the road texture contributions between wavelengths of a half millimeter and 50 millimeters is responsible for macro-hysteresis (majority of hysteresis present). Macro texture also plays a role in water drainage and runoff which is crucial in avoiding hydroplaning. Macrotexture is aided in this effort by the tread on tires which further adds to the capability of water drainage.

Surface Parameters

Eight surface parameters are used and widely accepted in industry to characterize the surface texture of a sample. These parameters are also often used as an approximate assessment for how much friction a surface can provide. Of these eight parameters two are significantly more

ubiquitous and utilized than the remainder. These two parameters are mean profile depth and surface roughness. Mean profile depth is calculated by using the equation shown below.

$$MPD = \frac{Peak\ 1 + Peak\ 2}{2} - Mean\ Value$$

This parameter is a way to characterize the depth by comparing the highest peaks in a row of surface data with the mean of that row. Surface roughness is governed by the equation below.

$$S_a = \frac{1}{A}\int_{X_0}^{X_n}\int_{Y_0}^{Y_n} |Z(x,y)|\, dx\, dy$$

This parameter is simply an arithmetic mean of all the height data points in a set of surface data. Both parameters are collected by companies and organizations in industry and considered when making repairs, replacing, and other safety and performance considerations.

Road Samples

Two types of road samples are utilized for testing in industry. Cores are samples taken by cutting a cylindrical sample out of a commercial road which is of interest. Pills are laboratory prepared cylinders. Pills are made by pouring all the necessary ingredients of a road composition into a gyratory compactor until a final pseudo-road sample is prepared. The two basic ingredients necessary to construct these pills are aggregates and binder. Aggregates are the chunks of different rock, either coarse or fine, that comprise the structure and friction abilities of a road. The binder is the material that holds the aggregates in place. In material science terms, The binder acts as the matrix while the aggregate acts as the reinforcement. Figure 3 shows a core on the left and a pill on the right.

Figure 3: Core vs. Pill

An easy way to differentiate the difference between cores and pills is the condition of the cylinder wall. Since cores are cut directly from road and aggregate intersects the boundary of cutting, exposed aggregate chunks can be seen on the cylinder wall. In the case of the pill all aggregate is constrained by the walls of the compactor meaning that binder will cover the entirety of the cylinder wall when pills are in new condition. Samples of both variations give companies the ability to test available friction, wearing, surface texture and other surface metrics in the lab without the hassle of coordinating road/lane closures and while avoiding the dangers of conducting tests on live roadways.

Previous Work

As noted in the acknowledgements, other engineering students at The Ohio State University laid groundwork crucial to being able to conduct the studies on this project. Previous work started with an inspection on correlating the eight surface parameters discussed above calculated from high resolution surface scans to available road friction. This study sampled 17 road surfaces with

two samples per surface. Once the eight parameters were determined form these samples, the surface was compared in whole as well as subsampled in an attempt to correlate the results to friction measured by British Pendulum Testing and Skid Tricks. No clear relationship could be drawn between the eight industry utilized and accepted metrics and the friction provided by each test surface.

Significant steps were then taken to improve filtering of these high-resolution scans. This portion of the previous work can be seen in chapter 2.

Guide to Thesis

Chapter 1 provides the motivation for the thesis. This chapter also contains some general and fundamental background information pertaining to the thesis. Lastly, this chapter contains a brief explanation of previous work. Chapter 2 discusses a study on the capability of the AMES 9500 RLTS. This begins with an introduction of more specific topics relevant to the study and previous work. The results of the study are then presented and are followed by the conclusions drawn from the study. Chapter 3 discusses a study which attempts to correlate state of wear of a surface to the corresponding change in friction. This begins with an introduction of more specific topics relevant to the study and discussion of a pilot study conducted previously. The results of the study are then presented and are followed by the conclusions drawn from the study. Chapter 4 recaps the conclusions from the studies detailed in chapters 2 and 3. Future recommendations are then discussed for each study. Future recommendations are also described for the FEM tire model introduced in Chapter 2.

Chapter 2: AMES Scanner Capability Study

Introduction

Objective

This study aims to assess the usefulness of the AMES9500 RLTS as a tool to examine the surface texture of rad profiles. This was tested by comparing a previously used tool, the AMES9300, to the 9500. Two samples were tested using both devices and the results were contrasted. The application for which this tool is being tested is generating a high-resolution surface profile for examination of surface texture. It will be determined that the 9500 is adequate if it is able accurately characterize the sloped microtexture region of the PSD plots and the macrotexture region. These features are important because this thesis attempts to relate the change in these textures over time (wearing) to available friction.

Laser Profilometry

One widely utilized way of characterizing surfaces is laser, or optical, profilometry. This method involves moving a high precision laser across a surface both laterally and longitudinally to determine the topography of the surface and create a 3D profile. This non-contact profilometry method is advantageous since it does not disturb the surface of interest which is especially useful on soft surfaces, surfaces where high precision is necessary, and surfaces with small peaks that are weak to shearing forces which could be applied by mechanical profilometry methods. Additionally, optical methods are able to bypass the aliasing that can be created by use of a stylus on a surface that has features much smaller in scale than the diameter of the stylus itself.

Laser profilometers (LP's) work by shooting a beam through a glass plate which is parallel to the surface of interest. Some portion of the beam is reflected by the plate and back to the measurement system. This establishes a datum for the height of the surface to be measured against. This datum is necessary because the LP works by measuring the relative distance between its glass plate and the surface rather than the surface height directly. The remainder of the beam which is not reflected by the plate contacts the surface of interest and is reflected to the measurement system. It is this disparity between reflections which is measured and used to calculate the surface profile as can be seen in the figure 4.

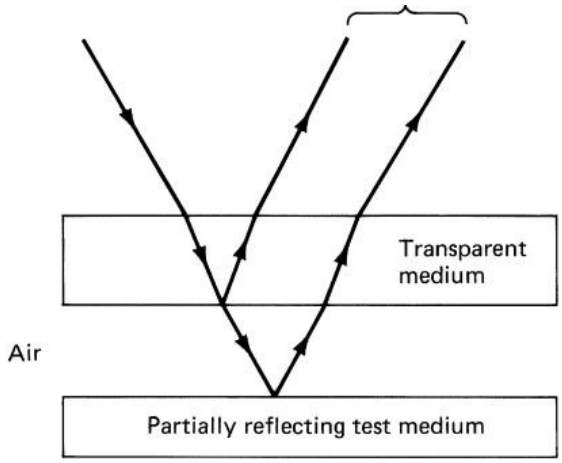

Figure 4: Working Principles of Laser Profilometers [1]

Two LP's have been used in the previous work on this project, the AMES LTS9300 and the AMES LTS9400HD. The 9300 utilizes a point laser to scan total surface of 107.95 mm length by 72.01 mm width. The max possible resolutions in the length and width directions are 15 μm and 63.5 μm, respectively, obtaining roughly 8 million data points in around 10 hours. The 9400HD also utilizes a point laser and has and identical scan area to the 9300. However, the 9400HD has max possible resolutions in the length and width directions of 6.35 μm and 24.7 μm respectively obtaining roughly 49 million data points in approximately 3.5 hours.

A new AMES product, the RLTS9500, may provide some advantages to the user over the 9300 and 9400HD. The RLTS9500 uses a line laser in order to cut down on scanning time at the cost of accuracy. The 9500 has a square surface area with sides of 101.6 mm. The only operating resolutions of the 9500's length and width are 49.6 μm and 41.5 μm respectively obtaining roughly 5 million data points in 90 seconds. A unit was obtained from AMES on loan in order to perform testing and determine if the lower resolution was still sufficient to capture the surface topology necessary for this project. The drastically reduced scan time would open many new doors for the project such as scanning an entire corner on a road or track.

Experimental Procedures

AMES LTS9300/9400HD

Since the 9300 and 9400HD have identical housing and external configurations, only one scanning fixture was necessary to test with each apparatus. The scanning fixture was placed on a datum plate and made parallel with the use of a level. This datum plate rested on vibration damping rubber pads and was measured to verify it was level. The fixture, datum plate, and level can be seen in the figure 5.

Figure 5: AMES9300/9400HD Scanning Fixture Setup [2]

Special care was taken to make the test fixture as parallel to the datum plate as possible. Taking this precaution helps prevent the data from showing a slope which is an artifact of the setup rather than a characteristic of the surface measured. After the test fixture is set for the given core/pill height and is leveled the scan settings were input. For this testing both scanners were run at 2916 lines over a surface area of 107.95 mm by 72.01 mm with maximum resolution in the width direction. The scan was then initiated, and the scanner was left still until completed. Upon completion the scan file was saved. Though the 9400HD is a more accurate and efficient machine, it was out of commission due to a battery issue at the time of this study. The 9300 was instead used as the benchmark against the 9500. The 9300 is still a capable machine and provided useful results for benchmarking.

AMES RLTS9500

The 9500 has a different size and shape than the 9300 and 9400HD as well as a different stilt system to suspend it above the desired work piece. Due to these differences, a new scanning fixture was required to test the 9500. A wooden board was cut to have a hole diameter of 6.25

inches in order for the 6 inch cores to fit. A few different sets of equal size blocks were then used in order to adjust the height of the board. This method was chosen over the more precise method of machining a new scanning fixture because the loaner 9500 obtained from AMES was only available for one work week. The scanning fixture can be seen in figure 6.

Figure 6: AMES9500 RLTS Scanning Fixture Setup

The scan settings on the 9500 are not adjustable. Each scan is performed at the machine's max resolution over a 101.6x101.6 mm square. The scan was then started, and the scanner left still until completion. When the scan was completed, the scan file was saved.

Scan Filtering

Spike errors are optical aliasing errors that can be found in optical profilometry measurements. These errors can be caused by highly polished aggregate causing inaccurate reflection measurements or different surface asperities such as cliffs shielding the laser from the actual surface in the valley past the cliff. Examples of spike errors can be seen in figure 7.

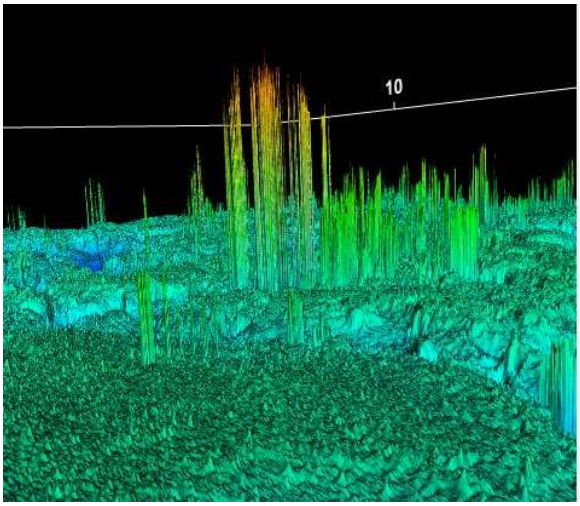

Figure 7: Spike Errors [3]

In order to account for these errors, the built-in MATLAB cumulative distribution function was used to create histogram plots for the height data contained in each scan. From these plots it was determined that the top 1% of data points were considered to be spike errors. After the cutoff height was established, the scan was split into a 9x9 grid and each sector was assigned an arithmetic average of all the points it encompassed. These grid sectors were then used as discrete data points to be input to the MATLAB Lowess fit function. Lowess is a locally weighted polynomial regression function which performs regression based on a weighting system established by the neighbors of each point of interest. This method was chosen due to its usefulness in situations where data is sporadic and has weak interrelationships between sections of data.

Once the new filtered surface was developed using the lowess function, the surface was suspended above the highest data point in the scan. It was then moved down toward the data by 1µm until the ratio of the data above the filtered surface is equal to the ratio of data above the cutoff height in the histogram. When this is achieved, all points lying above the filtered surface

and cutoff point are replaced with the value the filtered surface assigns for that location. The resulting surface is then saved as the filtered scan surface. Figure 8 shows this process in detail.

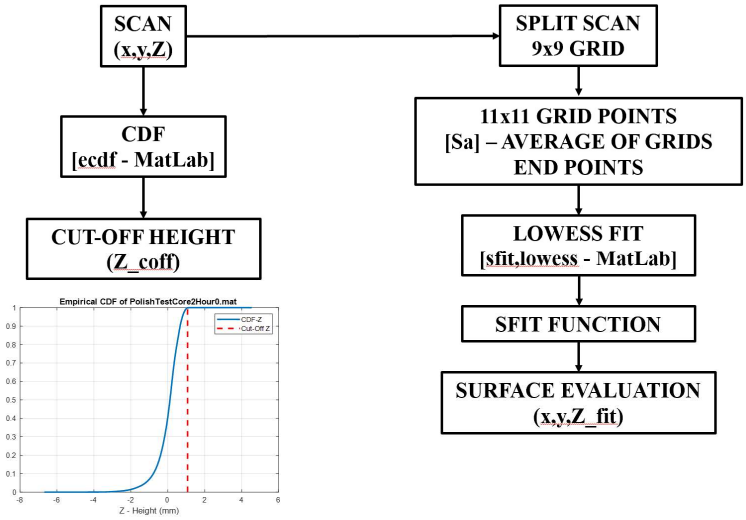

Figure 8: Filtering Method [3]

Data Chopping based on Tire FEM Model

Finite Element Method provides engineers the ability to simulate complex contact interactions by breaking the tire and road surface into finely meshed surfaces. This enables exploration of the complex deformation behavior that occurs at the interface. This is useful in studying tire-road interactions where the contact between the two surfaces occur on small asperities and are affected by textures with small wavelengths. This is also useful since the interaction on the contact patch does not propagate into the bulk behavior of the tire.

One metric which an FEM model could be useful to identify is actual contact area. Understanding how much of the tire is in contact with the road could allow for a significant portion of the scan data to be dismissed, since it is unlikely the tire would deform enough to fully

contact the lowest points measured in a scan. The immediate goal of the FEM work was to obtain an approximate measure of how much of the road surface will be contacted by the tire.

With a better idea of the real contact area, the unnecessary data can be removed, achieving two objectives. First, it may improve the correlation between surface characterization and friction available since points from the scan that the tire does not contact are effectively signal noise in the profile. Second, it drastically cuts down on analysis time for each scan.

A 2D tire contact FEM model was designed in Abaqus over a randomly distributed road profile. The tire is represented by a rectangle and is meshed with deformable 2D plane strain elements. A downward load was applied to the top of the tire until the applied pressure reached 24 psi, the standard used for the skid trailers which are utilized to obtain friction measurements of surfaces. Results over ten surface profiles showed a contact area that was between 20% and 30% of the full tire area available to contact the road. One of the models tested can be seen in figure 9.

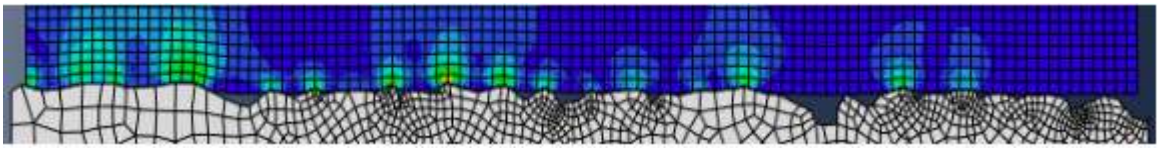

Figure 9: FEM Tire Model in Contact with Road Profile [4]

To account for this, data was removed from the bottom up from the filtered scan. All points below the top 20% and 30% of data were replaced by a flat surface. A flat surface was chosen in order to keep from changing the surface parameters calculated.

Power Spectral Density Plots

Many pieces of literature in tire-road inspection have shown power spectral density (PSD) plots to be useful in assessing the frequency content of road profiles. PSD plots are obtained by taking

the Fourier transform of the autocorrelation function applied to a data set. In this project the built-in MATLAB functions fft and pwelch were used to carry out PSD calculations. PSD plots help visualize the contribution to a profile by different wavelengths and how the power of the road spectrum is represented over its fundamental wavelengths. Characteristics of this curve that were considered during this experiment are the area under the PSD plot and the slope of the non-horizontal portion of the plot. Area under the PSD plot is significant because the integration under the PSD curve results in the total power of the scanned surface. This is important because two pills of the same aggregate and binder recipe will still have different powers, which may be attributable to different performances of each surface tested. The slope of the non-horizontal region is significant because it shows how sharply the contribution by lower wavelengths falls off and how much mircotexture is present.

Two important metrics of PSD plots are area under the curve and, in the case of road surfaces, the slope of the microtexture region. The area under the curve in a PSD plot is equal to the root mean square of the profile. This is used as a mean profile metric and is used as a new mean parameter to define the surface texture. This is used in light of the mean profile depth mentioned in Chapter 1 since previous work displayed no correlation between MPD and friction. The slope of the microtexture region is important because it defines the amount of microtextrure that is available on a surface. A less negative slope results in a higher percentage of the signal being attributed to microtexture, while a more negative slope means less microtexture.

Core Choices

Two cores were chosen to perform the capability test for the 9500. Due to other work required of the 9500 in the week it was on loan and the slow scan time of the 9300 it was being compared to,

only two cores could be compared. However, the entire core library was scanned using the 9500 to be available if it is determined that the 9500 is adequate.

The first core chosen was core 33. Core 33 is a hydroblasted pavement with coarse aggregate which was obtained from the Transportation Research Center (TRC). This core was chosen because it is more randomly distributed than the other cores in the library and did not have any surface characteristics that were caused by influences outside of the road's initial construction or normal wear and tear. Core 33 can be seen in figure 10.

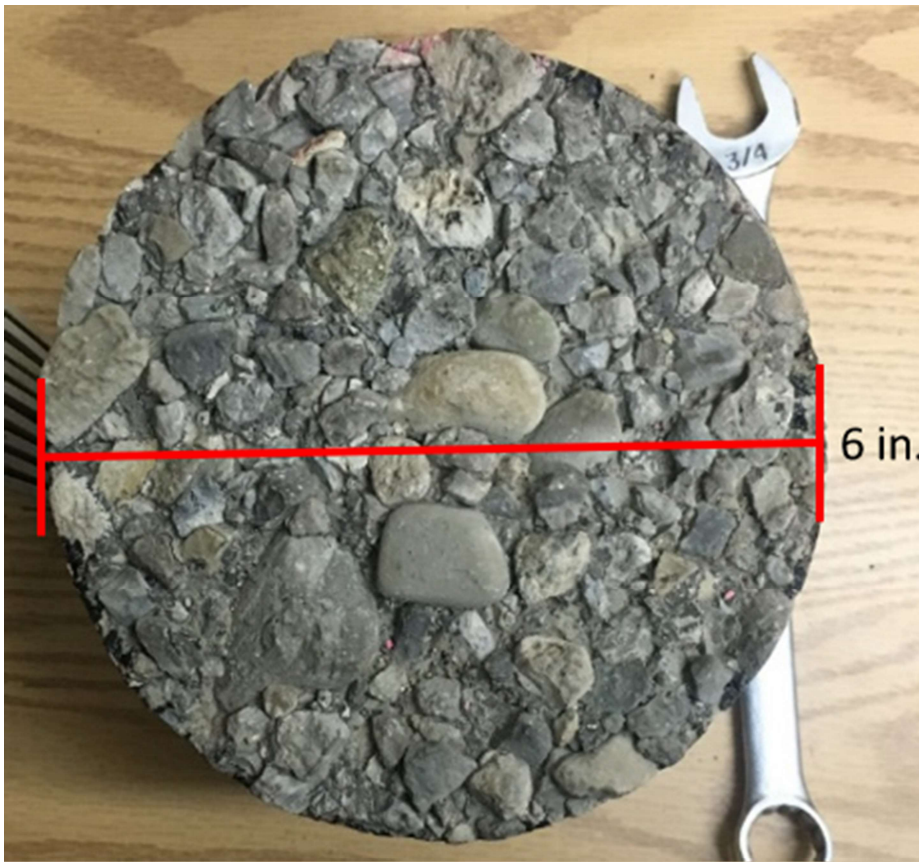

Figure 10: Core 33

The second core that was chosen was core 16. Core 16 is a concrete surface which had been ground and grooved as reparative measures. This core was obtained from a state route which has heavy traffic. Core 16 can be seen in figure 11.

Figure 11: Core 16

This core was chosen because of the obvious effect of repair on the surface and its heavily influenced distribution. This surface also represents a highly spike error prone surface due to the large and numerous cliffs on the surface resulting from the grooving of the concrete. This core will test the ability of the 9500 to retain minimal errors with its lower resolution relative to the 9300 and will determine if the lower resolution is unable to capture microtexture after surface treatments such as diamond grinding.

Results and Discussion

Scan Characteristics

Due to the low precision setup used to scan with the 9500, both scans had plateaus in the corners due to scanning off the core. This was corrected by removing the first and last 298 lines from the scan. This reduced the scan size for each scan from 101.6x101.6 mm to 101.6x72 mm. This did

not affect core 33 since the distribution was random and a large enough majority of the scan area was intact so that aliasing due to one asperity or group of asperities was not an issue. This also did not affect core 16 since the lines were cut off perpendicularly to the grooves on the surface. This means that the contribution to the PSD of the grooves is retained and changed negligibly in magnitude. As with core 33, enough of the scan was intact to avoid aliasing of larger asperities.

The scan of core 33 performed by the 9300 was partially corrupted during data transfer. A portion of the data became erased and the last 766 of 2916 lines had to be removed from the scan resulting in a new scan width of 53.0835 mm. This result is suboptimal but should not affect this study since the scan areas of the two machines are already inherently different and a majority of the data was retained.

Since the surfaces created by the data chopping procedure in accordance with the FEM tire model are artificial, this section will only report the results associated with these surfaces. The analysis will focus on the filtered and unfiltered surfaces.

Core 33

Core 33 was scanned using both apparatus, filtered, and the PSD of the surface was plotted. The resulting PSD plot from the 9300 benchmark can be seen in figure 12.

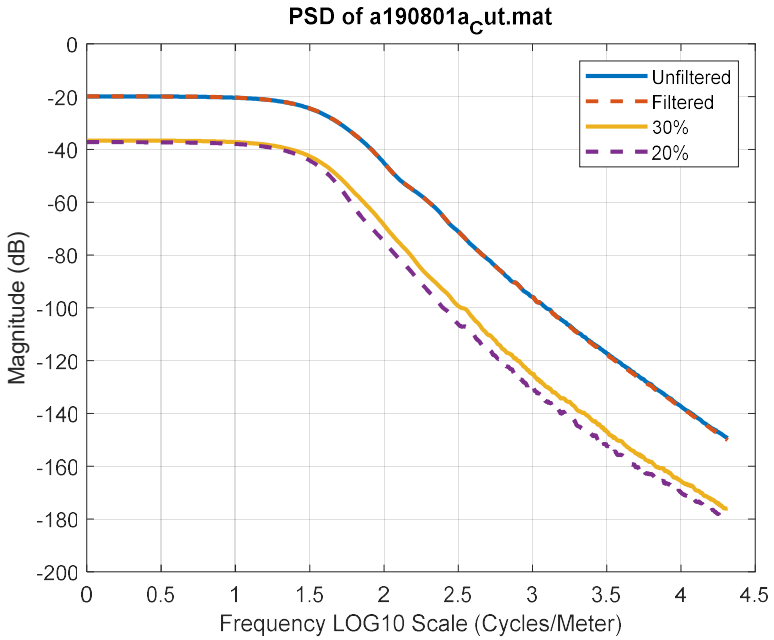

Figure 12: Core 33 PSD from 9300 Scan

The PSD plot from the 9500 can be seen in figure 13.

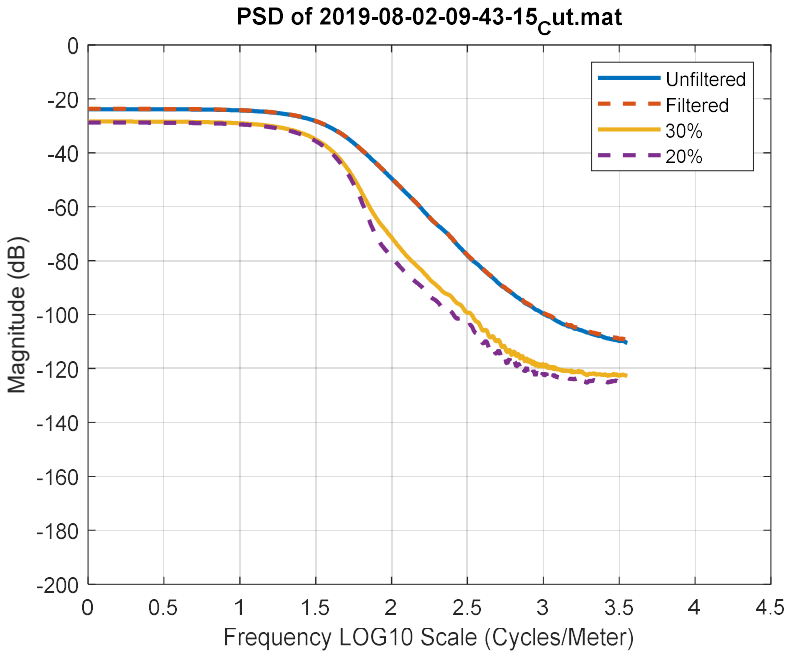

Figure 13: Core 33 PSD from 9500 Scan

It is apparent from these figures that there are significant differences between the 9300 and 9500 scan results. The magnitude of the flat portion of the graph for the filtered and unfiltered lines on the 9500 are a little lower than that of the 9300. This disparity is small, however. Note that in both graphs the break from horizontal to negative sloping behavior occurs at about the same location around 1.5 cycles/meter. Over the first .5 cycles/meter of the sloped region both graphs decay about 20 decibels. The slope is preserved until about 2.5 cycles/meter where it begins to diverge from the slope of the 9300 scan. The data recorded by the 9500 stops about .8 cycles/meter before the 9300. This chunk of missing data from the 9500 was expected since it has a lower scan resolution in both the width and length so it cannot capture as short of wavelengths as the 9300.

Figure 14 and 15 show windows of the PSD plot focusing on the sloped region.

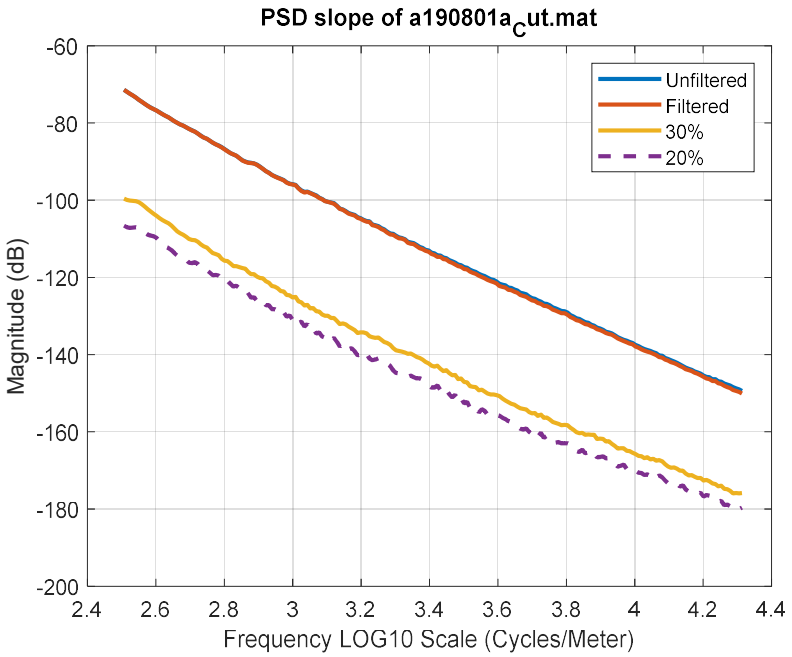

Figure 14: Slope Region for Core 33 from 9300 Scan

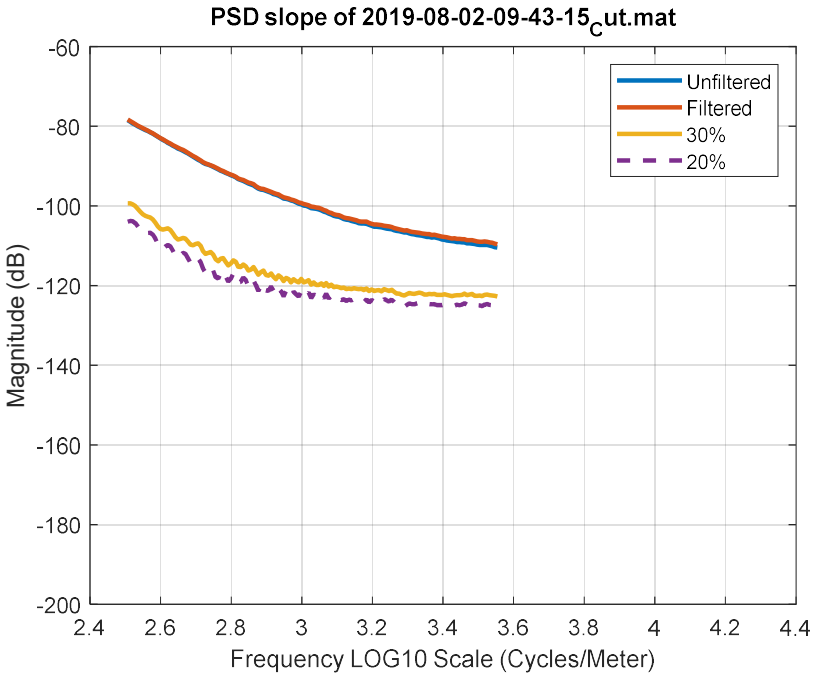

Figure 15: Slope Region for Core 33 from 9500 Scan

As noted above, the slope of the 9500 diverges quickly from that of the 9300 and cuts off early. It is expected that with a randomly distributed surface, the sloped region will be purely linear. Note that this is essentially true of the filtered and unfiltered portions of the 9300 benchmark scans. This linearity is lost in the 9500 scan which seems to asymptotically towards -120 dB.

Tables 1 and 2 below show the calculated slope of the best fit line to the sloped region, and the area under the PSD curve.

Table 1: Core 33 Metrics from 9300 Scan

Core 33: 9300 Metrics				
Data Set	Unfiltered	Filtered	30%	20%
Area	-204.147	-204.666	-256.212	-265.692
Slope	-42.455	-42.7988	-42.2979	-40.9959

Table 2: Core 33 Metrics from 9500 Scan

Core 33: 9500 Metrics				
Data Set	Unfiltered	Filtered	30%	20%
Area	-104.135	-103.713	-123.544	-127.05
Slope	-30.5391	-29.8309	-20.0936	-17.8099

Note that the loss of data over the range from roughly 3.5 to 4.4 cycles/meter on the 9500 plot resulted in almost halving the area under the PSD. The leveling off of the sloped region in the 9500 also resulted in around a 12dB/Cycle/meter change in slope.

Since the magnitude of the horizontal region is very similar between graphs and exhibits identical trends, it is apparent that performance in the sloped region will be the determining factor in the usefulness of the 9500.

Core 16

Core 16 was scanned using both apparatus, filtered, and the PSD of the surface was plotted. The resulting PSD plot from the 9300 benchmark can be seen figure 16.

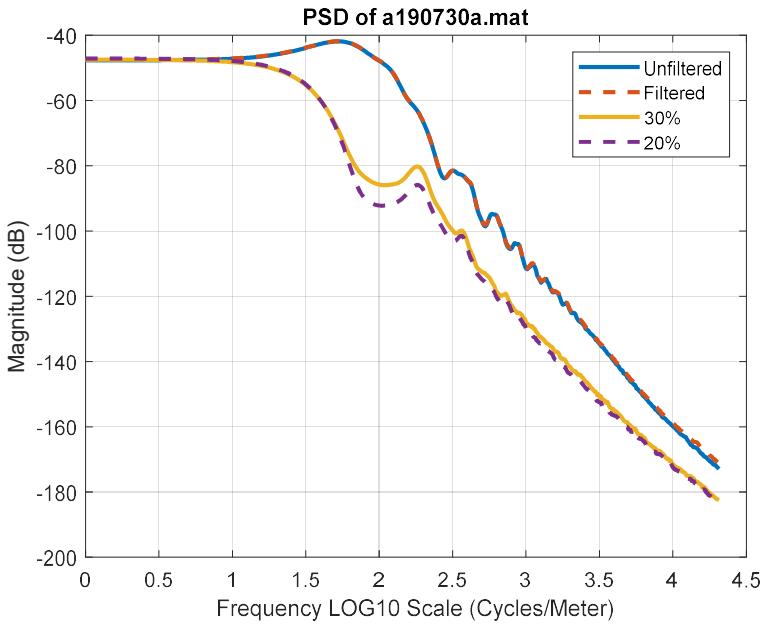

Figure 16: Core 16 PSD from 9300 Scan

The PSD plot from the 9500 can be seen in figure 17.

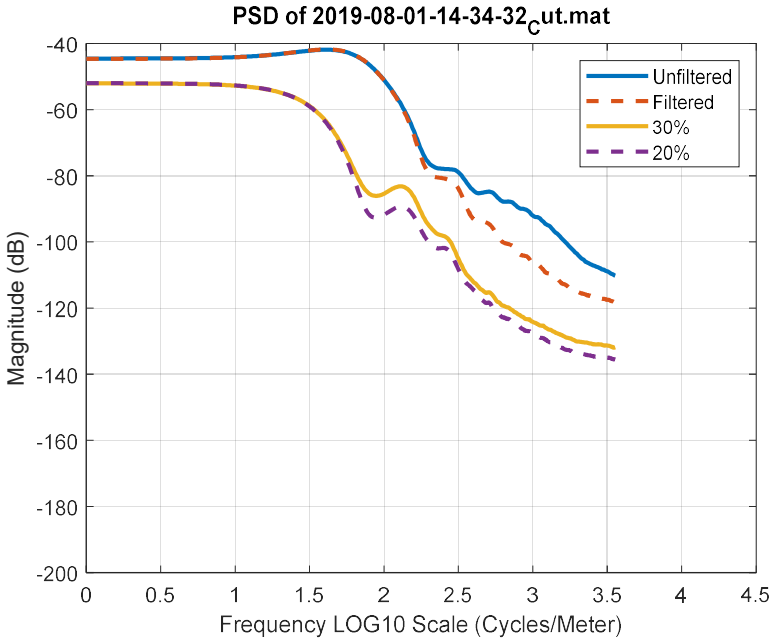

Figure 17: Core 16 PSD from 9500 Scan

From visual inspection of the graphs it can be seen that the 9500 is able to see the phenomena caused by the grinding and grooving. Also apparent from visual inspection, the 9500 is unable to maintain the trend with the filtered data. This may either be a problem with the 9500, or a break in robustness of the filtering code due to the nature of the surface chosen. Since the filtered and unfiltered portion of the PSD's for core 33 correlate nearly perfectly, it will be assumed that this is a filtering algorithm issue. Again, it is noted that the magnitude of the pre-slope region is similar between the two machines and even through the first big parabolic asperity which is caused by the large ruts left by grooving processes.

The slope regions are windowed and shown in figures 18 and 19 below.

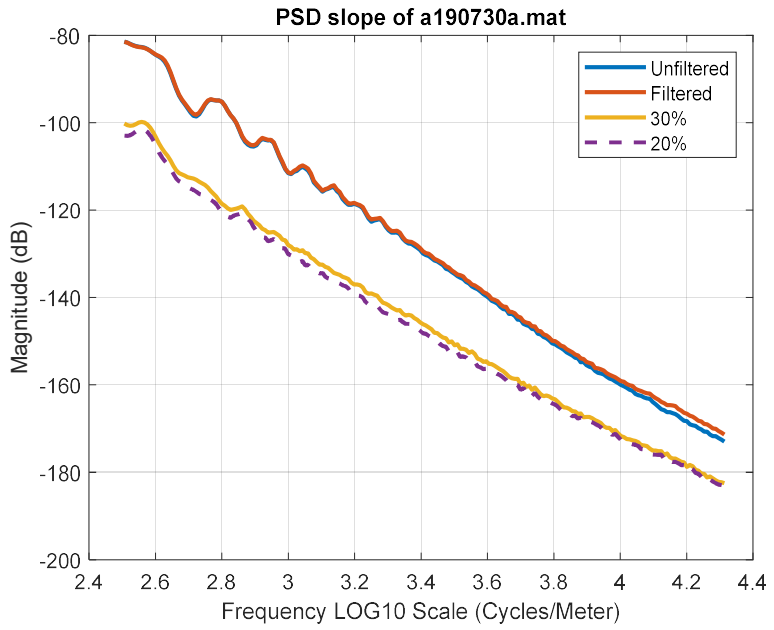

Figure 18: Slope Region for Core 16 from 9300 Scan

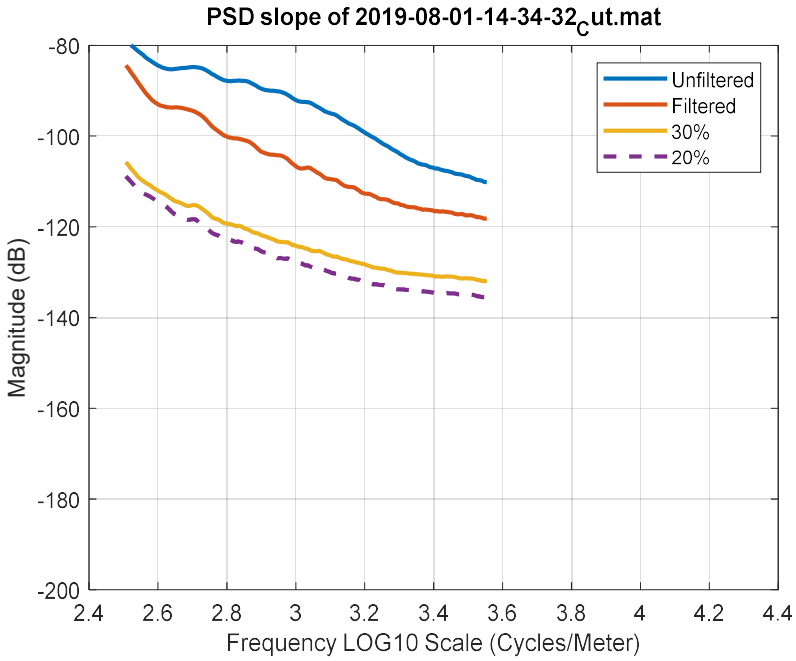

Figure 19: Slope Region for Core 16 from 9500 Scan

The 9500 did not reproduce the slope region demonstrated by the 9300. As seen in the 9300 slope region, though sinusoidal, a fairly linear decreasing trend can be observed. Though decreasing, the 9500 slope is irregular in shape and does not exhibit a slope similar to the 9300.

The metrics for both scans of core 16 can be seen in tables 3 and 4.

Table 3: Core 16 Metrics from 9300 Scan

Core 16: 9300 Metrics				
Data Set	**Unfiltered**	**Filtered**	**30%**	**20%**
Area	-234.698	-233.654	-262.778	-265.702
Slope	-51.191	-50.3513	-45.4122	-44.5341

Table 4: Core 16 Metrics from 9500 Scan

Core 16: 9500 Metrics				
Data Set	Unfiltered	Filtered	30%	20%
Area	-100.136	-112.032	-130.551	-134.217
Slope	-29.6168	-30.9055	-23.2964	-24.1337

Note that due to the high disparity between the sloped regions the area for unfiltered and filtered scans for the 9500 is less than half that of the 9300. Note that the slope has about a 20 dB/cycle/meter difference between machines.

Conclusions

On Core 33 the 9500 was able to sufficiently reproduce the pre-slope region of the PSD plot in both magnitude and trend. For this core the 9500 was able to reproduce the slope region for a small band of frequencies just after the pre-slope region. On Core 16 the 9500 was able to sufficiently reproduce the pre-slope region and the large anomaly caused by grooving. The 9500 was not, however, able to reproduce the sloped region for this core. For both cores metrics had large disparities between machines.

The 9500 showed promise for roads that have not been altered after construction and have more random surfaces such as Core 33. The 9500 showed troubling results for roads that have unnatural surface asperities such as ruts from grooving. More work is required to determine the capability of the 9500. Future work suggestions for this study can be found in Chapter 4.

Chapter 3: Polishing Study

Introduction

As a road surface is traveled on, aggregate is ripped up, smoothed, sheared, etc. All of these interactions caused by driving over a surface greatly affect the micro and macrotexture of the surface, thus changing the friction provided by the surface. This interaction can be simulated in the lab by forcing contact and movement between a road sample and rubber in order to create polishing. This polishing represents a portion of the aging that is experienced by a real roadway. Other factors which affect aging of roadways that are not considered in this study are temperature cycling, adverse weather, pollutants, etc. A previous pilot study of polishing was completed and showed promising results that apparent friction changes occurred over polish time as well as significant changes in topology of the pill surface. The results of this pilot are discussed later in the chapter before the presentation of the results of this study. This study sought to draw a meaningful connection between the change in available friction of a surface and the change in its surface topology.

Experimental Procedures

Scanning using the AMES LTS9400HD

The AMES LTS9400HD was used as the LP for this study. The 9400HD has a scan surface area of 107.95 mm by 72.01 mm with resolutions resulting in 49 million data points. The 9400HD takes around 3.5 hours to complete a full resolution scan.

The scanning rig used in chapter 2 was again used for this study. All scanning procedures remain the same with the added step of marking the pills and datum plate to ensure that the orientation of the pill was as repeatable as possible in each scan.

British Pendulum Tester

The British Pendulum Tester (BPT) is an apparatus which swings a rubber pad attached to the end of a pendulum arm over a surface of interest. A pin which is guided by the pendulum stops at the peak of the pendulum's path. This pin is located directly behind the pendulum and is pushed along its path until the pendulum falls. The pin remains at the peak position of the pendulum. A scale from 1-160 is present in the area where the pin stops in order to categorize the amount of friction which acted on the rubber pad. The numbers on this scale are known as British Pendulum Numbers (BPN). A higher BPN correlates to more friction. The exact change in friction associated with a unit BPN change is widely debated and believed to vary with surface type. One floor friction organization's standard for slip testing acknowledges that changes in these numbers do not give rise to an obvious standard and rather groups BPN numbers into groups labeled by risk level. [7] This type of method is also used by organizations that deal in road safety. The BPT used for this study can be seen in figure 20.

Figure 20: British Pendulum Tester

Before each round of testing, the pendulum was allowed to swing without a contact surface in place. The sensitivity or the rotational bearing was varied until three straight successful 0 BPN runs could be made. After calibration the pill of interest was dusted off in order to remove any loose aggregate or foreign particles which may affect the BPN readings.

In order to ensure repeatability a 3 inch by 5 inch rectangle was marked on the top of the pill. The corners of this rectangle were continued down the side of the pill so that its location could be recovered after each polishing step. An arrow in symbol was also marked on the side of the pill to illustrate the travel path of the BPT. An example of the rectangle marking can be seen in figure 21.

Figure 21: Pill for Polishing Showing BPT Rectangle

At the beginning of each test the rubber pad was brought flush with the 3-inch side of the rectangle. A trial test was conducted to check the condition of the setup and then 4 live test runs were conducted. The average of these runs was taken and reported as the final BPN for the test.

This test was completed in both wet and dry conditions. The test was first conducted wet since polishing is a wet operation and the BPN was obtained immediately after polishing. The pill was wetted with distilled water before each pendulum swing. After drying, the test was completed dry using the same methodology of repeatability and calibration discussed above, excluding wetting.

The Polisher

The device used in this study, appropriately named The Polisher, uses a cylindrical rubber pad to simulate wear caused by a tire. This pad is brought to contact the sample and rotates for a set duration. The Polisher can be seen in figure 22.

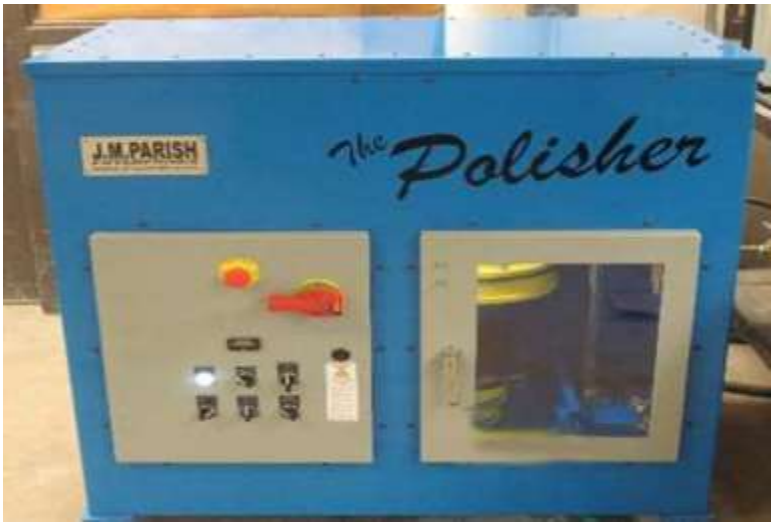

Figure 22: The Polisher

The polishing is done in a wetted environment to promote longevity of the polishing pad and to keep temperatures low during contact to avoid adhesion between the sample and the rubber. The water feed was kept at 120 cc/min.

There are some inherent sources of error with The Polisher. Since the outside of the rotating pad is moving faster than the inside, the pill is polished unevenly with rate of polish being a function of radius. At the center of the pad there is little to no rotation which results in a static downward pressure acting on a circle at the middle of the sample. This phenomenon results in a divot about the diameter of a quarter manifesting over time.

Another error source is caused by the lack of a method for aggregate that comes loose during polishing to escape from the pill. The aggregate gets forced into the rubber pad and effectively becomes a cutting tool in a lathing operation. This results in an annular rut forming on the surface of the pill.

Lastly, the equivalence between a unit amount of polishing time on The Polisher and traffic wear in a real-world application in unknown. Since the tire contact patch is only in contact with a

given location on a road surface for a fraction of a second, polishing occurs over months and years rather than minutes and hours. For example, a tire moving at a longitudinal velocity of 60 mph will rotate a 5 inch contact patch away from the road surface in 4.73 milliseconds.

Pilot Study

Three pills of an identical asphalt mix were created to be polished. Each of these three pills was polished in half hour intervals twice for a total of 1 hour on each pill. The BPN of the pills was recorded before testing and after each half hour interval. Figures 23 and 24 below show the dry and wet BPN results for pills A, B, and C.

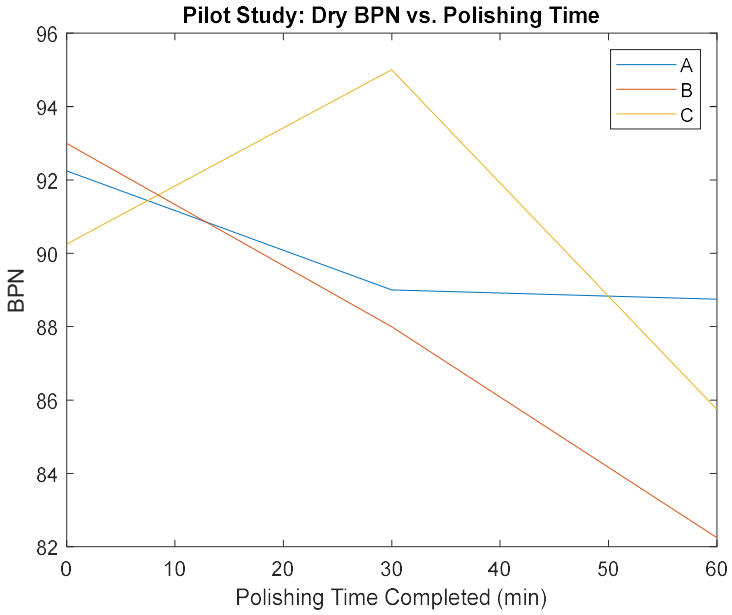

Figure 23: Pilot Study Dry BPN vs. Polishing Time

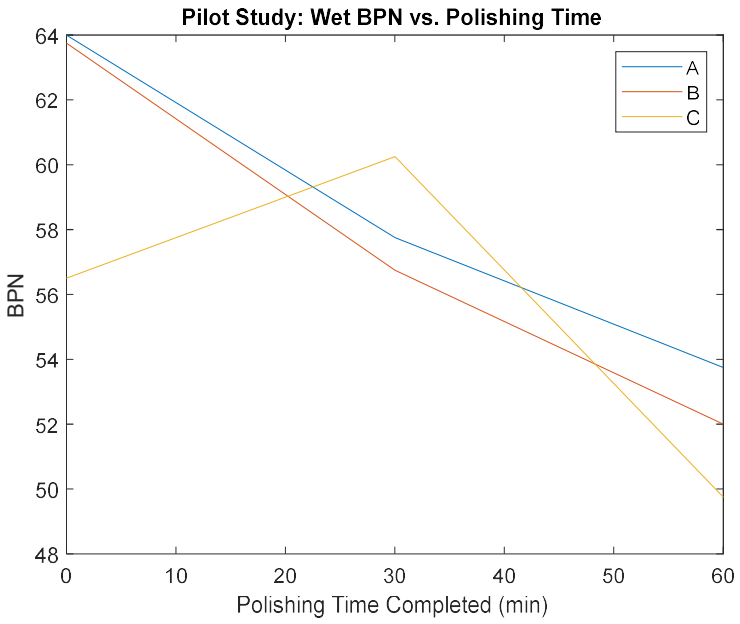

Figure 24: Pilot Study Wet BPN vs. Polishing Time

These figures show that The Polisher is able to create a significant change in the surface of a pill and thus a change in available friction. It is unclear why pill C exhibited behavior significantly different than that of pills A and B. To try to eliminate this error extensive future care will be taken to ensure BPN repeatability. This is most likely the source of error since the pill construction process is used by organizations for safety testing and had been deemed acceptable to produce repeatable and accurate samples of road for testing.

Testing Sample and Specifications

Two of the pills from the pilot study were used for testing in this study. Since the pills are generally homogeneous, with the exception for a slight tendency of one end to have larger aggregate due to the effects of gravity during compaction, the flip sides of pills A and C were used. These new samples are referred to as pill Y for the flip side of C and pill Z for the flip side of A.

Each of these pills were polished in 15 minutes intervals for a total of two hours. After each polishing session, the pills were tested on the BPT in both dry and wet conditions and scanned.

Results and Discussion

Outliers

From analyzing the BPN and PSD data, two points in the data were identified as outliers. One of these can be seen in figure 25, which shows a plot of area under the PSD curve vs. wet BPN. The point that has a much higher area than the others is the identified outlier.

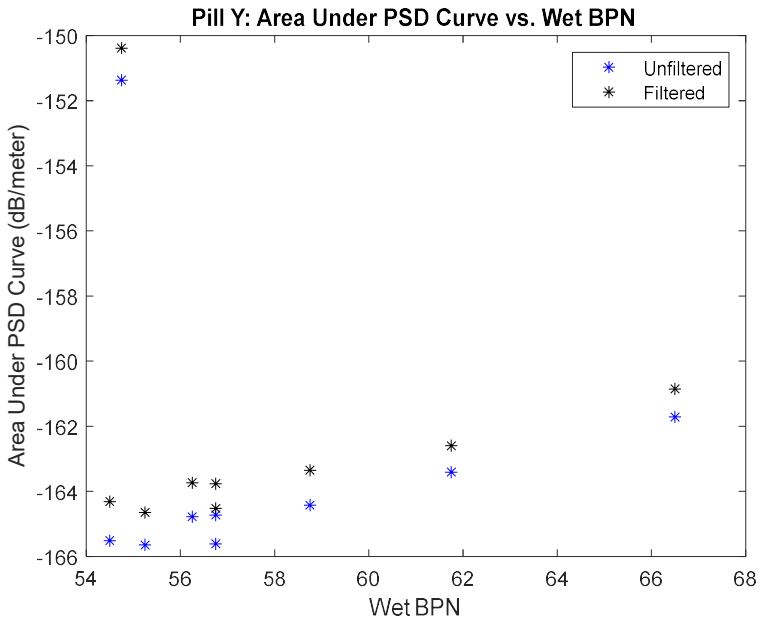

Figure 25: Outlier for Pill Y

The data point for 1 hour and fifteen minutes of polishing on pill Y and the data point for 1 hour and 45 minutes on pill Z were outliers. Upon inspections of the scan files and scan renderings in the AMES software, it was noted that these outliers were caused by problems with the scanner during data. The anomalies seen in these scans are believed to have been caused by the fact that

the pads which run along the tracks for the laser were going bad and may have caused mechanical errors.

The results presented in this section have had these outliers removed and they will not be discussed.

Also note that pill Y has a pre-polishing data point while pill Z does not.

Visual Inspection

MATLAB was used in order to replot the scan images over a normalized color map. The progression over the polishing period for pill Y can be seen in figure 26 below. The figure should be read increasing time left to right, then top to bottom. Due to the outlier removal and starting at different times this figure is meant to display a general trend in the change over time rather than a step by step representation which will be examined in plots generated later in this chapter.

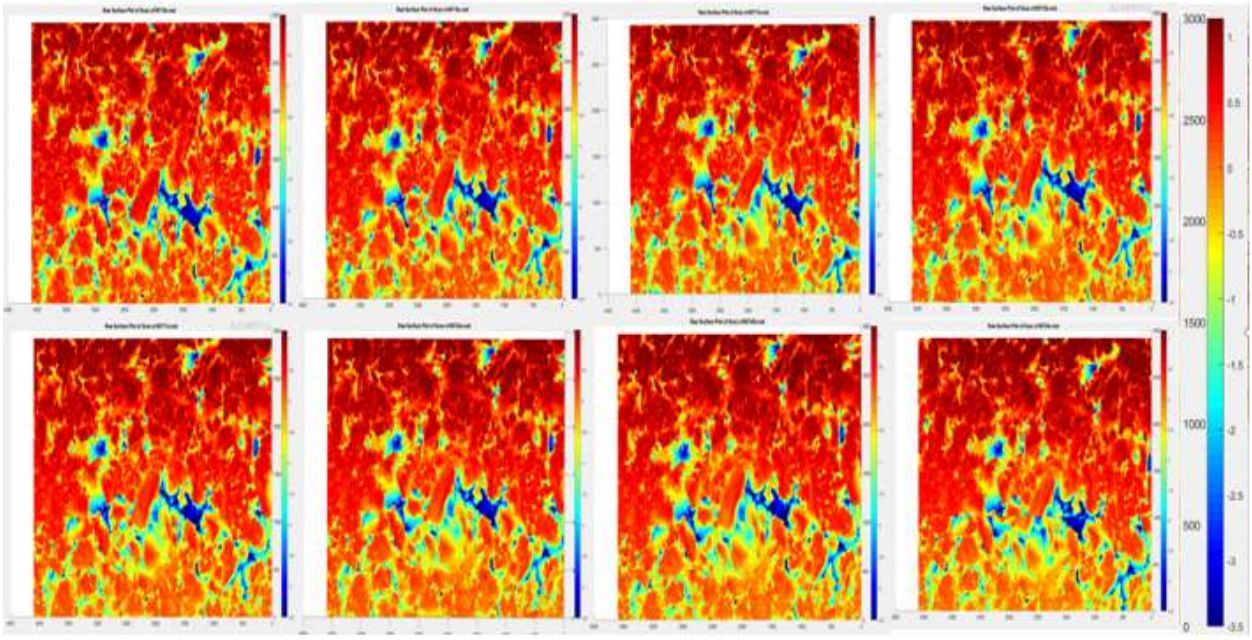

Figure 26: Pill Y Visual Inspection of Polish Over Time

It was noted from this plots that there were changes in the asperities on the surface of the samples. This can be most obviously noted by the rectangular piece of aggregate near the middle of each image. Notice that this aggregate chunk goes from a consistent dark red to lighter and inconsistent red/orange. This shows two things: First, the chunk polishes over time, and second, the chunk polishes unevenly along its surface.

Pill Y

Pill Y was polished in 15-minute intervals for a total of two hours. Pill Y also has a data point before polishing. The BPT results for both wet and dry conditions can be seen in figures 27 and 28 including error bars for variance between the four runs that were averaged for each test.

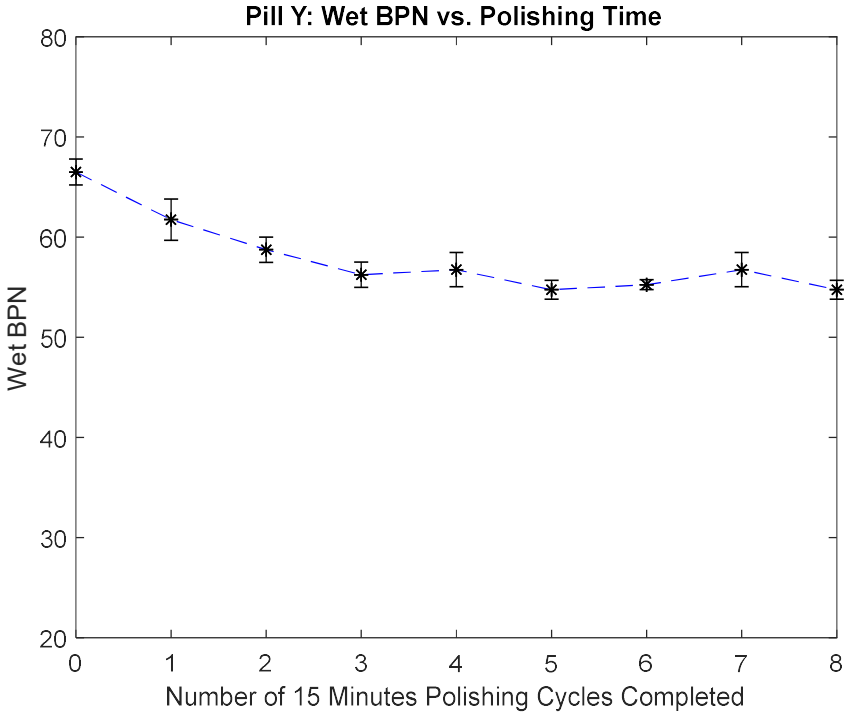

Figure 27: Pill Y Wet BPN vs. Polishing Time

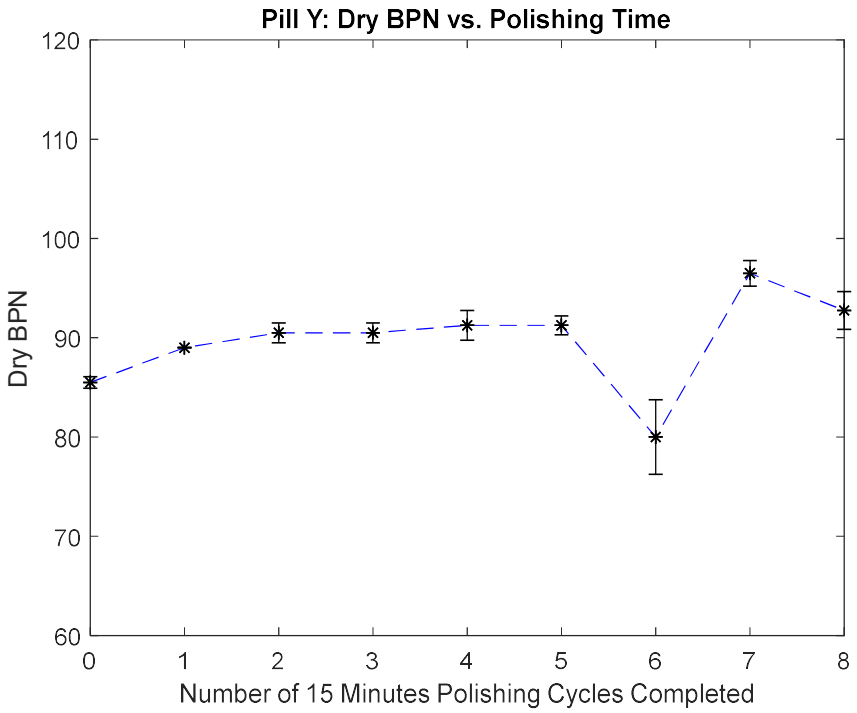

Figure 28: Pill Y Dry BPN vs. Polishing Time

Note that wet BPN decreases with time. Dry BPN starts by increasing which is presumed to be due to the removal of binder from the surface and exposure of fresh aggregate. After this it could be that a "rip and polish" phenomenon occurs. This is where a chunk of aggregate is ripped off the surface of the pill exposing new and rugged surface in its place. This new surface adds available dry friction due to the addition of microtexture. After this new location is revealed, further polishing time smooths the region and removes available friction from the surface.

The PSD's of these scans were plotted for each polishing interval. The area under the PSD curve as well as the slope were plotted against dry and wet BPN as well as polishing time to inspect the correlation between surface topology and available friction.

This method was completed for the unfiltered scan, the filtered scan, and the scans with data removed based on the FEM tire model discussed in Chapter 2. Figure 29 and 30 show the area

under the PSD curve against polishing time. In these figures an apparent negative trend exists between area and increasing polishing time.

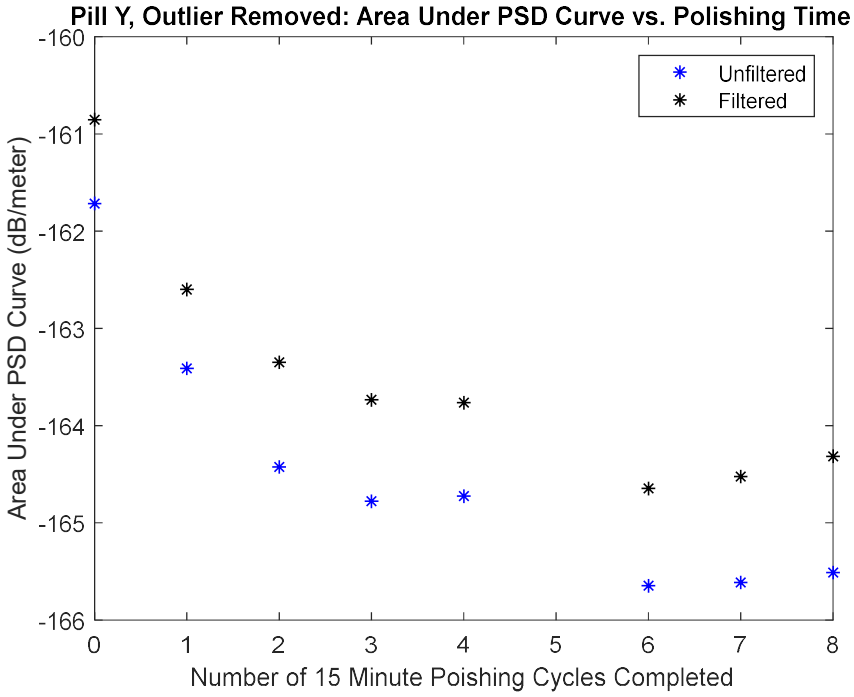

Figure 29: Pill Y Area Under PSD Curve vs. Polishing Time; Unfiltered/Filtered

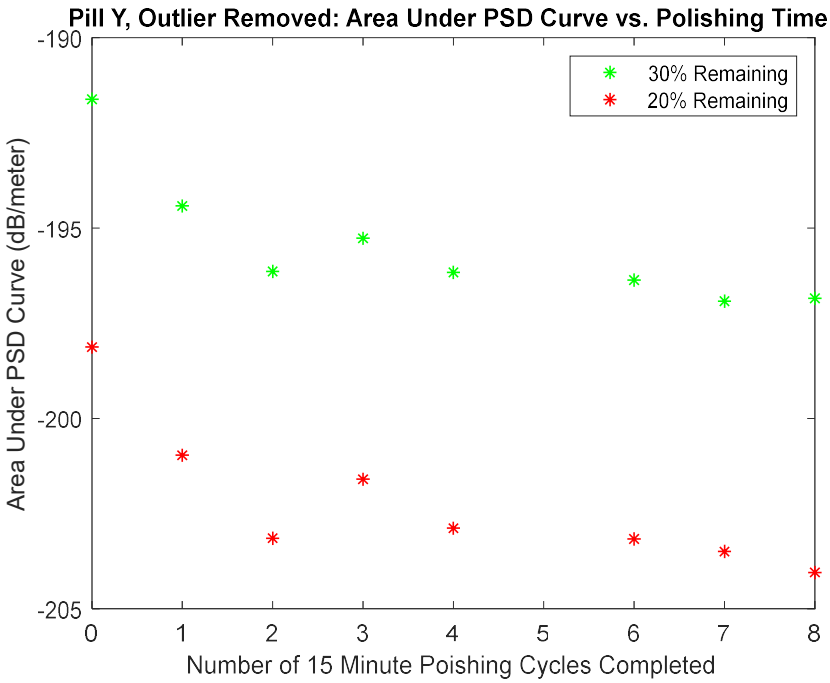

Figure 30: Pill Y Area Under PSD Curve vs. Polishing Time; Data Removed

Figures 31 and 32 show PSD slope against polishing time. Note that a negative trend similar to that seen for area under PSD curve is exhibited by the data for the unfiltered and filtered cases. This trend, however, is not apparent for the 30% and 20% data remaining cases.

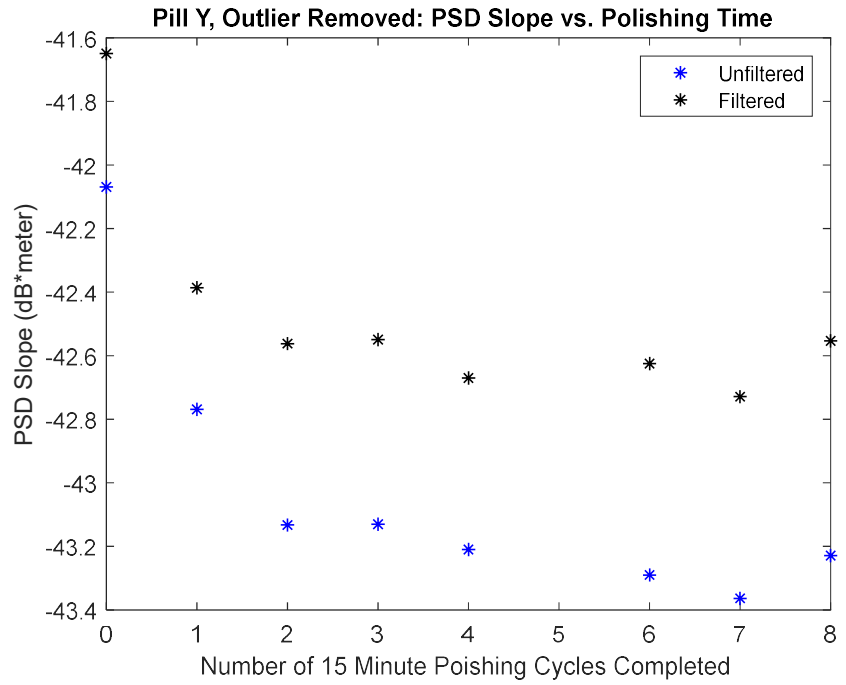

Figure 31: Pill Y PSD Slope Curve vs. Polishing Time; Unfiltered/Filtered

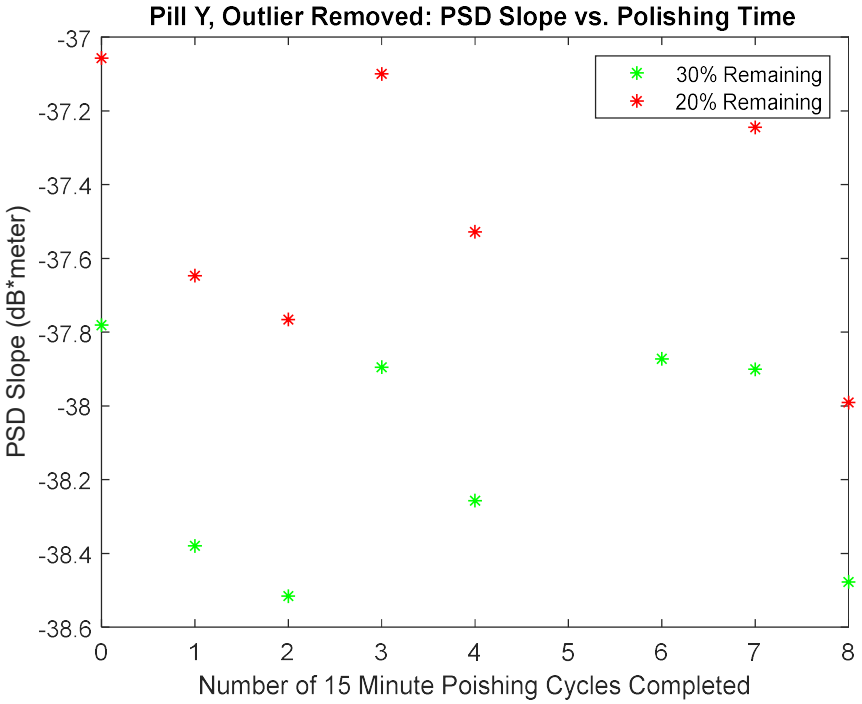

Figure 32: Pill Y PSD Slope Curve vs. Polishing Time; Data Removed

Figures 33 and 34 show the area under the curve against wet BPN. A fairly apparent positive trend between area and increasing wet BPN can be seen.

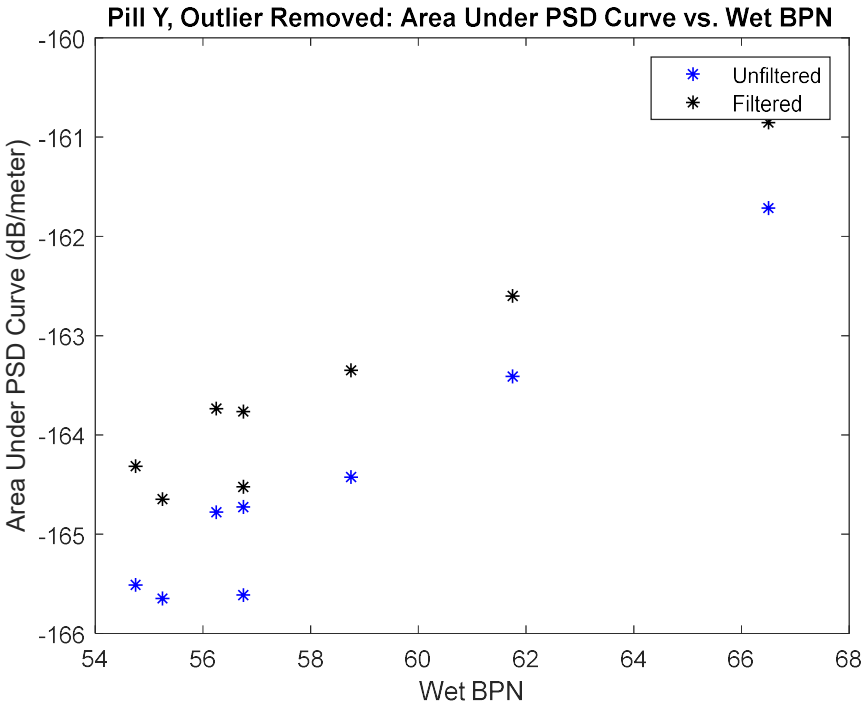

Figure 33: Pill Y Area Under PSD Curve vs. Wet BPN; Unfiltered/Filtered

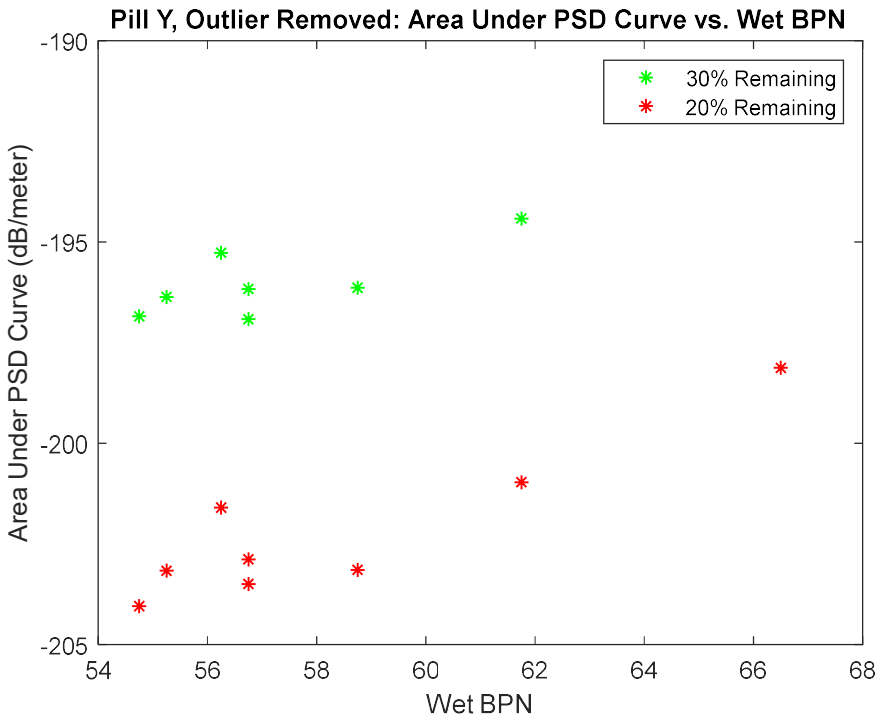

Figure 34: Pill Y Area Under PSD Curve vs. Wet BPN; Data Removed

Figures 35 and 36 show PSD slope against wet BPN. Note that a positive trend similar to the one exhibited in the area vs. wet BPN graphs can be seen in the cases of unfiltered and filtered. In the cases of 30% and 20% data remaining, no clear trend is apparent.

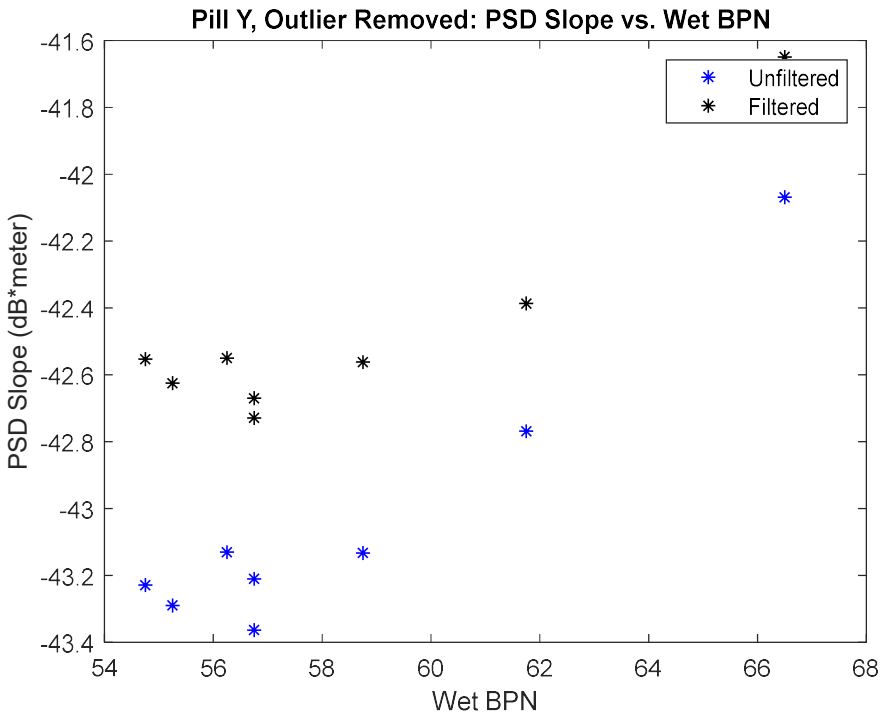

Figure 35: Pill Y PSD Slope vs. Wet BPN; Unfiltered/Filtered

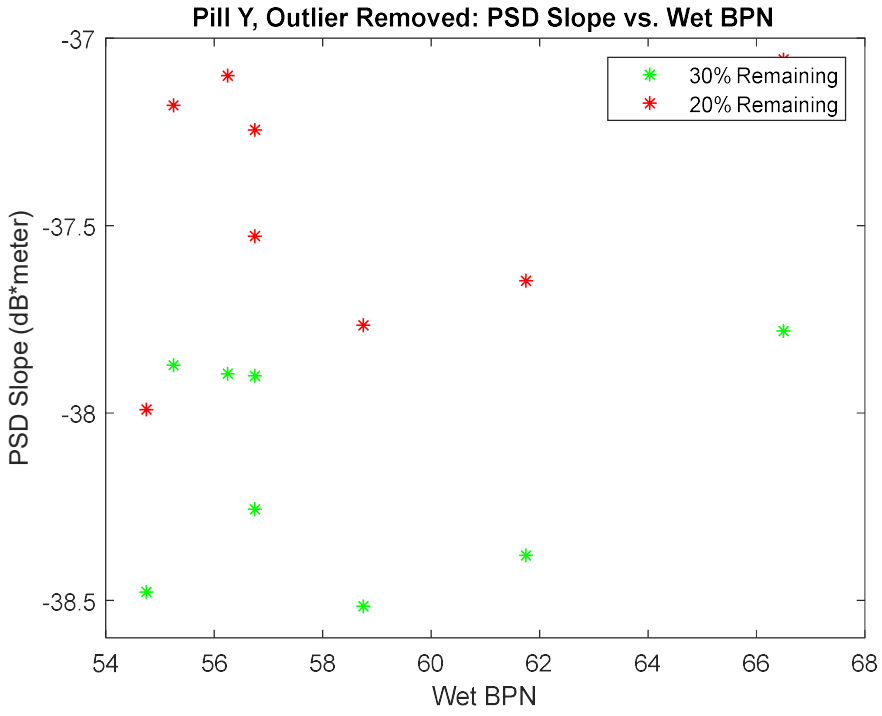

Figure 36: Pill Y PSD Slope vs. Wet BPN; Data Removed

Figures 37 and 38 show area under the PSD against dry BPN. Note that in all cases, with the exception of the outlier at 80 BPN, a clear negative trend can be seen between area and increasing polishing time.

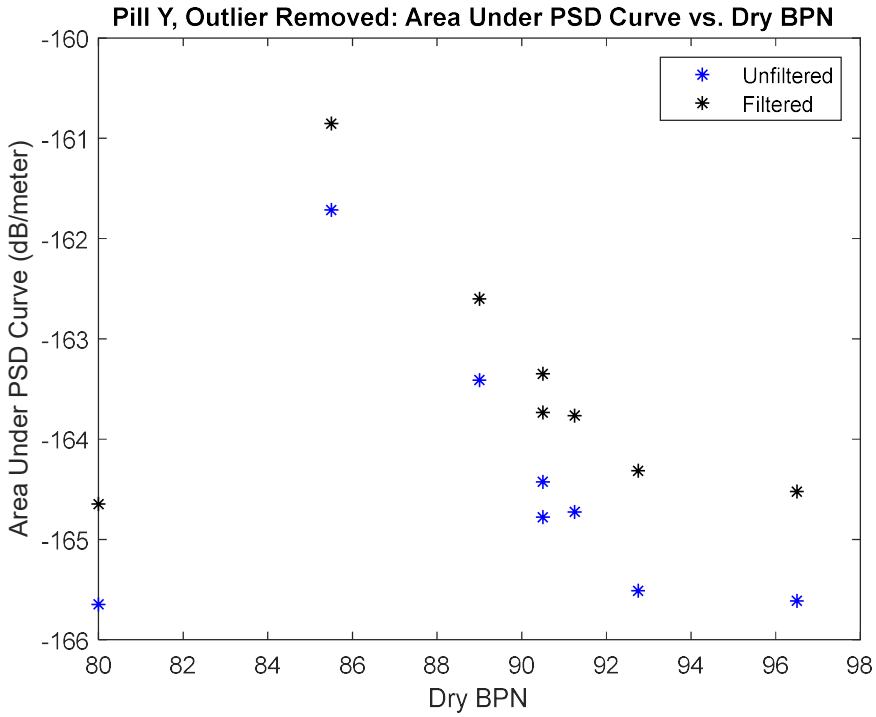

Figure 37: Pill Y Area Under PSD Curve vs. Dry BPN; Unfiltered/Filtered

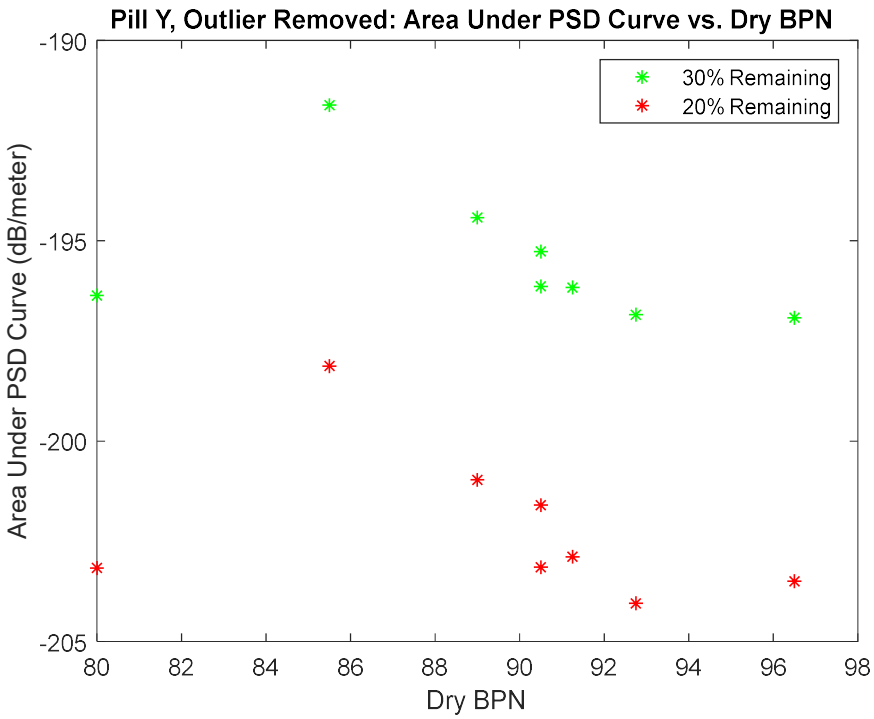

Figure 38: Pill Y Area Under PSD Curve vs. Dry BPN; Data Removed

Figures 39 and 40 show PSD slope against dry BPN. Note again that the negative trend can be seen in the unfiltered and filtered cases with the exception of the outlier. Both data removal cases did not exhibit any clear trend.

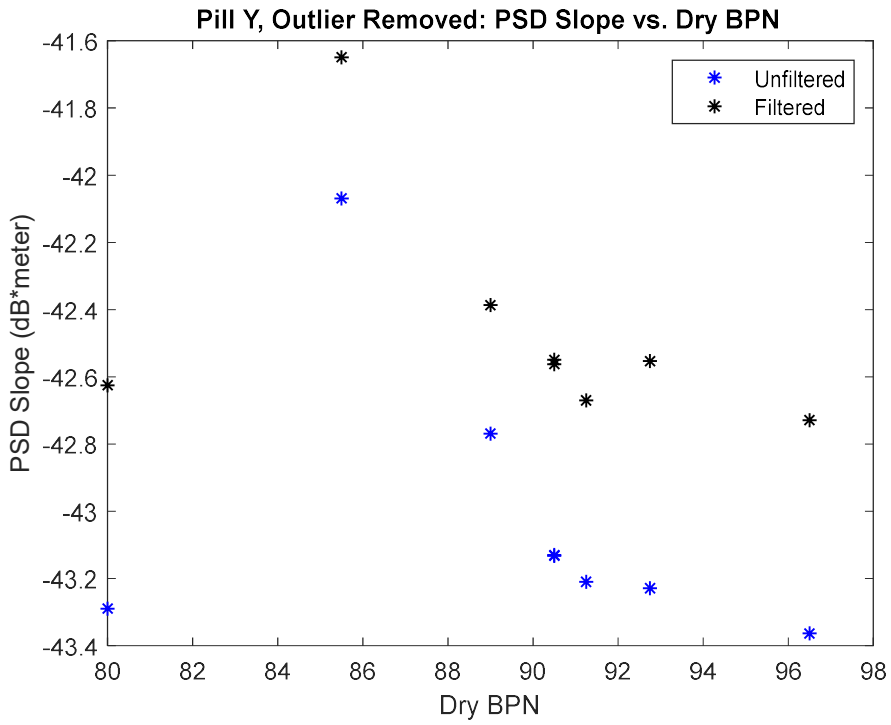

Figure 39: Pill Y PSD Slope vs. Dry BPN; Unfiltered/Filtered

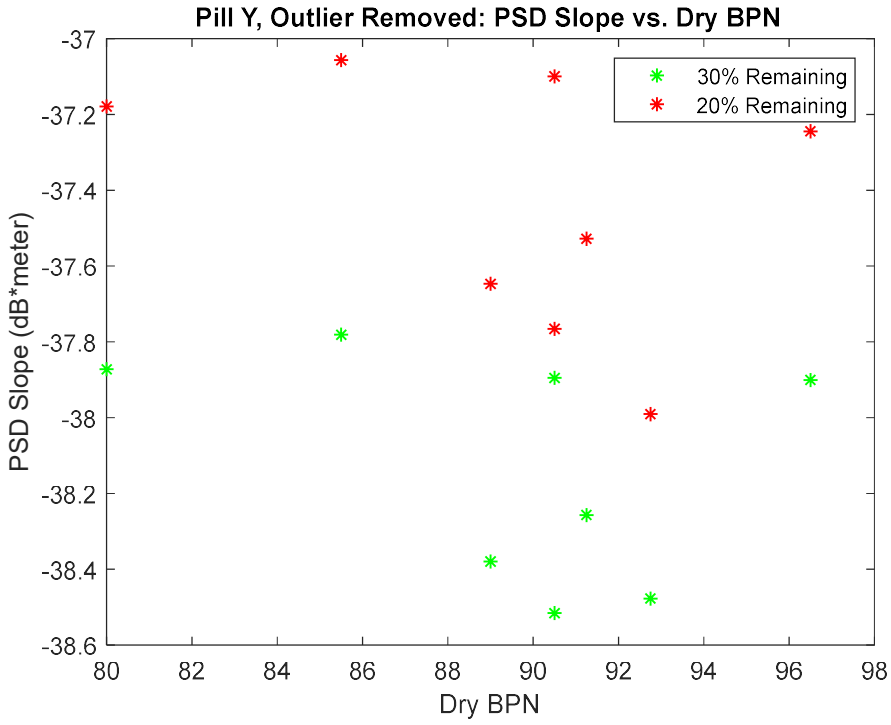

Figure 40: Pill Y PSD Slope vs. Dry BPN; Data Removed

Pill Z

Pill Z was polished in 15 minute intervals for a total of two hours. Pill Z does not have a data point before polishing. The BPT results for both wet and dry conditions can be seen in figures 41 and 42 including error bars for variance between the four runs that were averaged for each test.

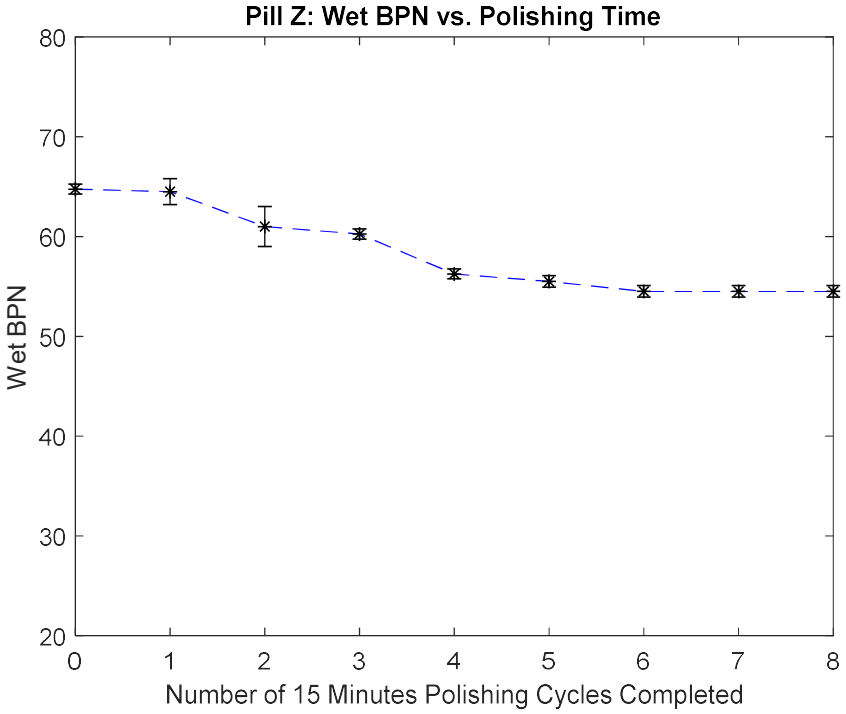

Figure 41: Pill Z Wet BPN vs. Polishing Time

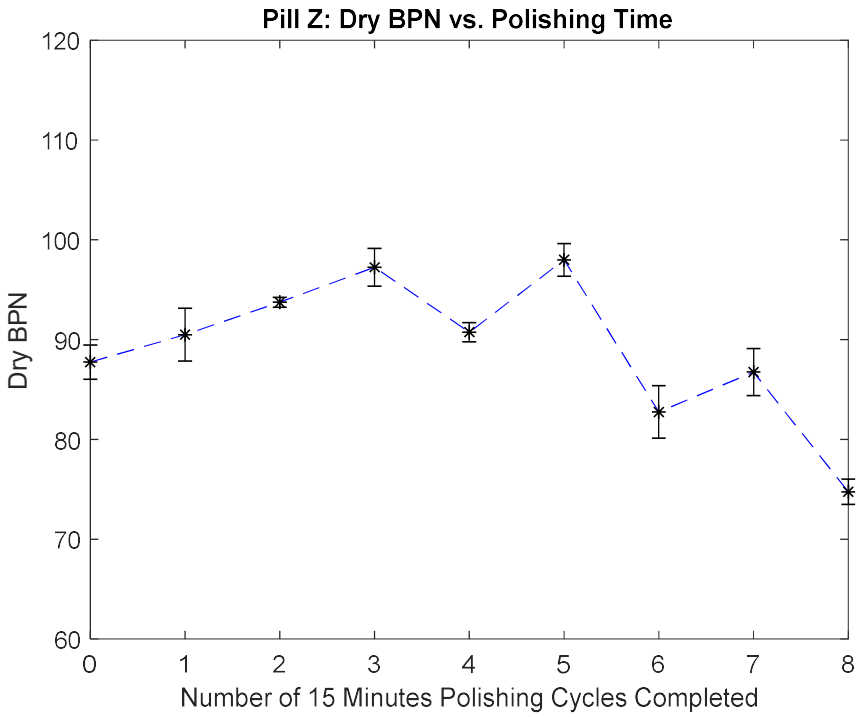

Figure 42: Pill Z Dry BPN vs. Polishing Time

Note that again there is a steady decrease in available friction vs polishing time in the wet conditions. Again, the dry conditions initially have an increase in BPN. For dry BPN for pill Z the "rip and polish" behavior is very apparent.

Figures 43 and 44 show the area under the PSD against polishing time note that no clear trend can be seen for any cases.

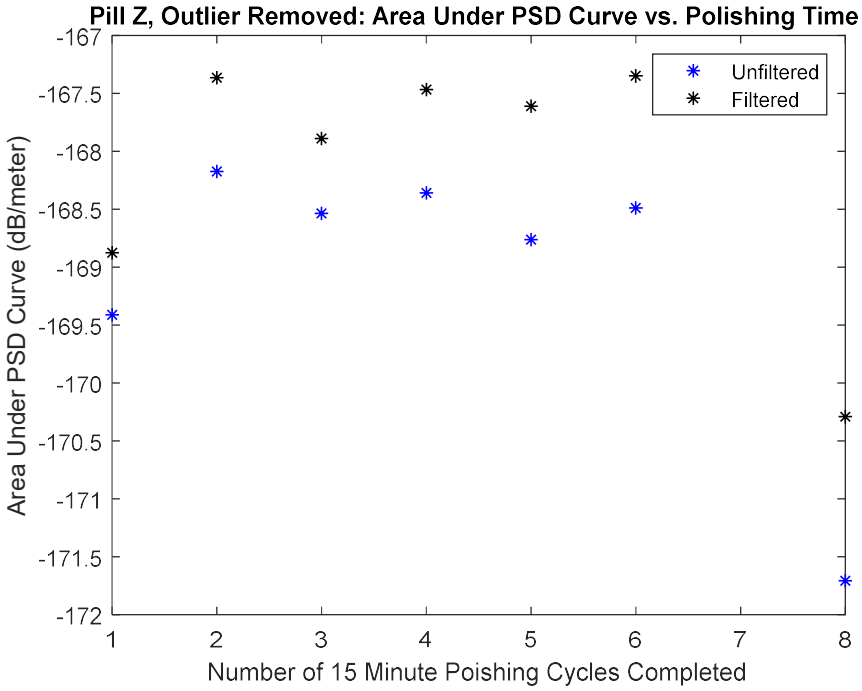

Figure 43: Pill Z Area Under PSD Curve vs. Polishing Time; Unfiltered/Filtered

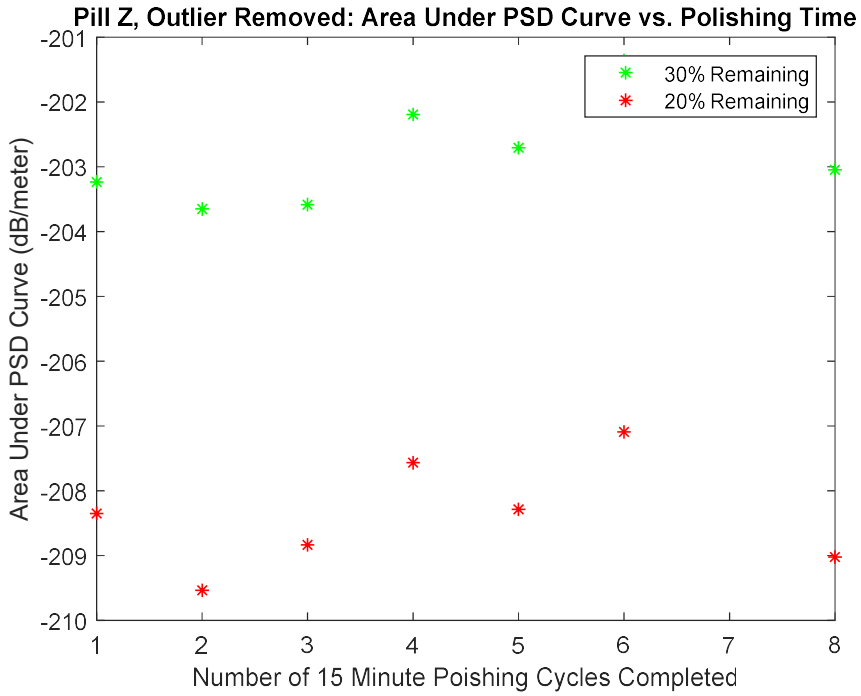

Figure 44: Pill Z Area Under PSD Curve vs. Polishing Time; Data Removed

Figures 45 and 46 show PSD slope against polishing time. Note that no clear trend can be seen in all cases.

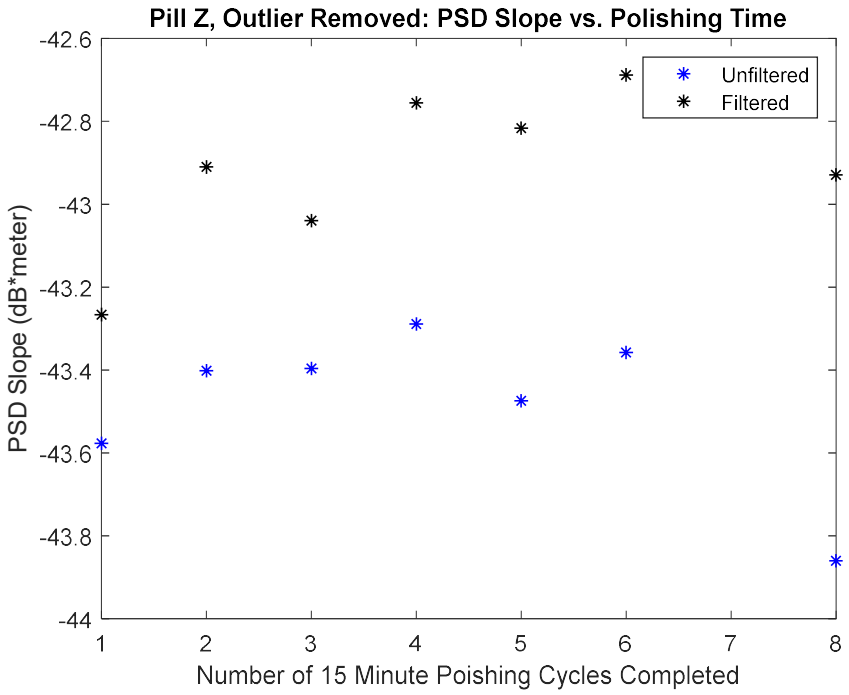

Figure 45: Pill Z PSD Slope vs. Polishing Time; Unfiltered/Filtered

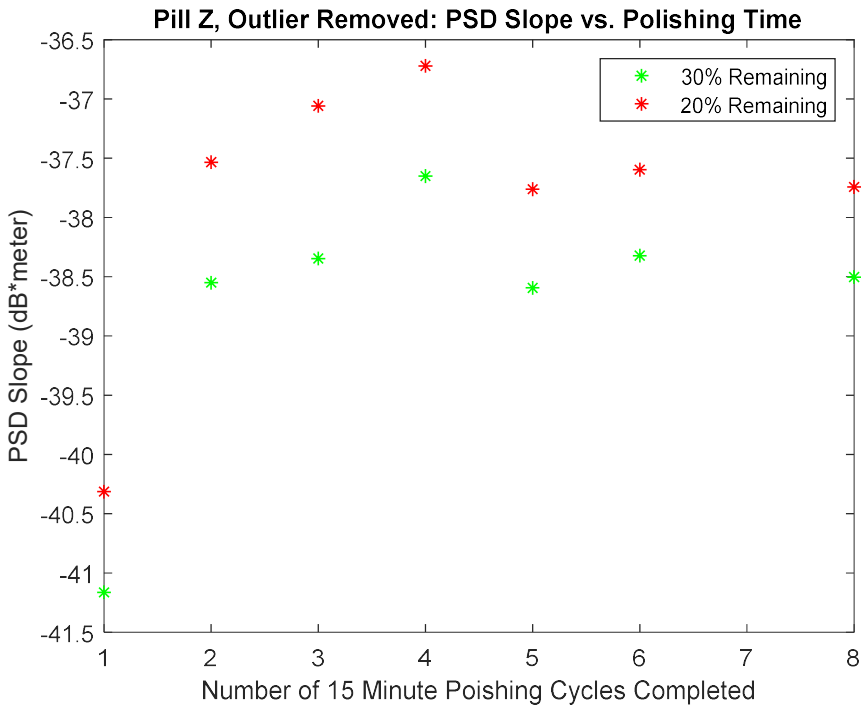

Figure 46: Pill Z PSD Slope vs. Polishing Time; Data Removed

Figures 47 and 48 show area under the PSD against wet BPN. Note that no clear trend can be seen.

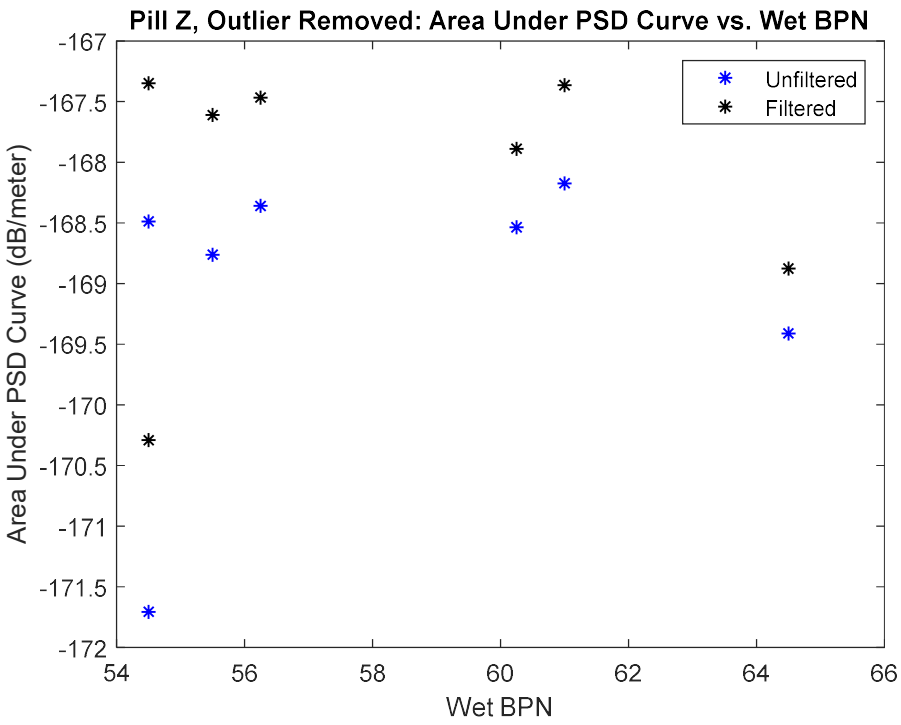

Figure 47: Pill Z Area Under PSD Curve vs. Wet BPN; Unfiltered/Filtered

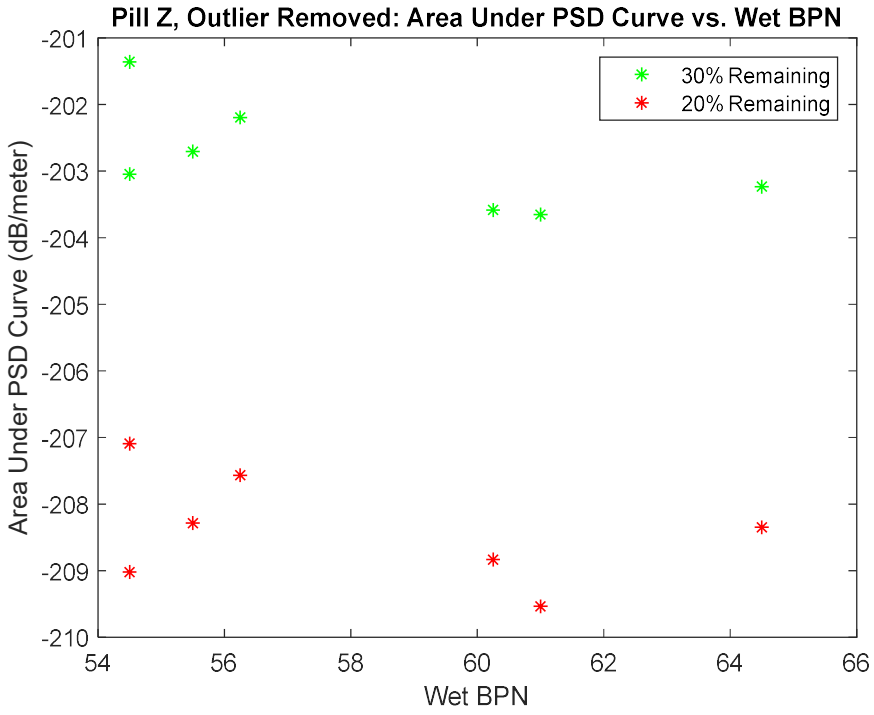

Figure 48: Pill Z Area Under PSD Curve vs. Wet BPN; Data Removed

Figures 49 and 50 show PSD slope against wet BPN. Note that no clear trend can be seen.

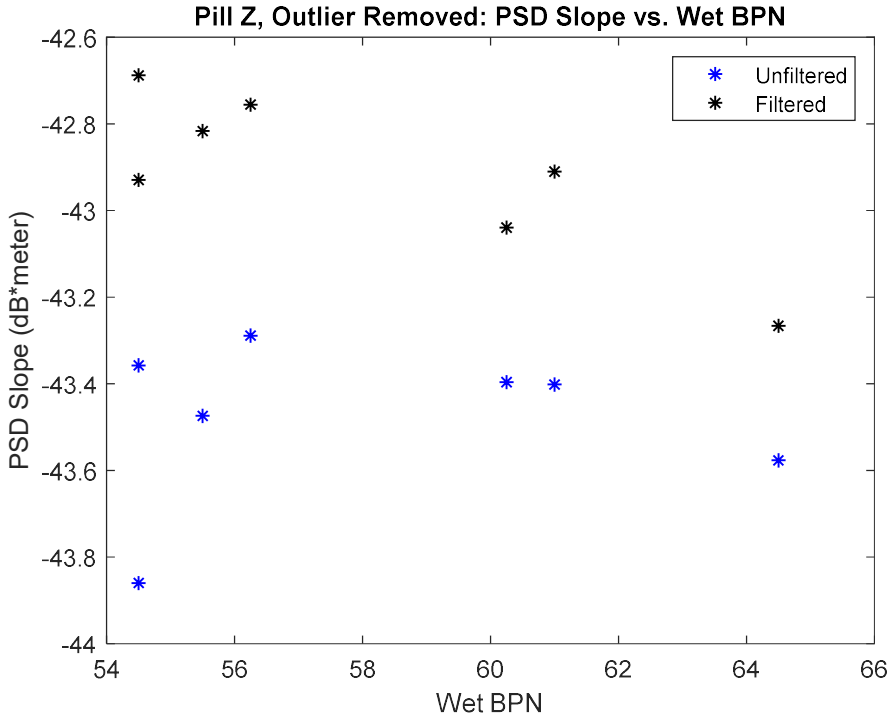

Figure 49: Pill Z PSD Slope vs. Wet BPN; Unfiltered/Filtered

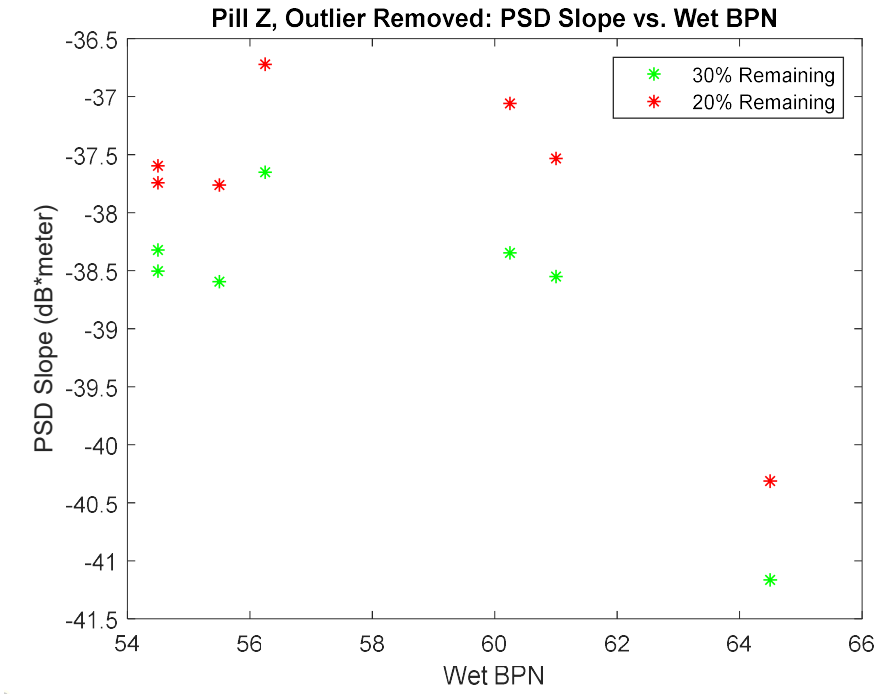

Figure 50: Pill Z PSD Slope vs. Wet BPN; Data Removed

Figures 51 and 52 show PSD slope against dry BPN. Note that no clear trend can be seen.

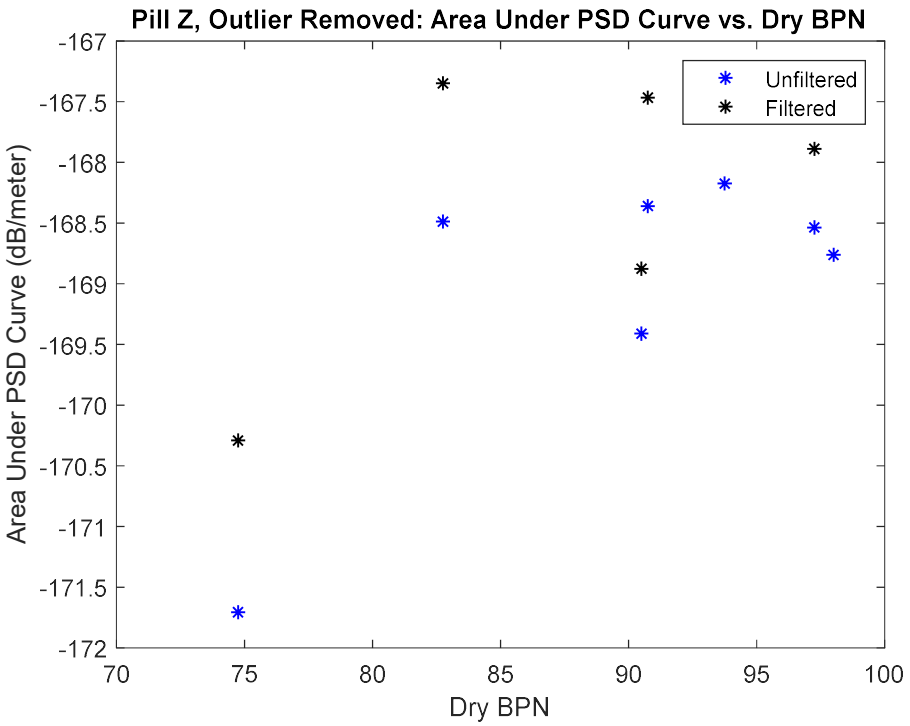

Figure 51 Pill Z Area Under PSD Curve vs. Dry BPN; Unfiltered/Filtered

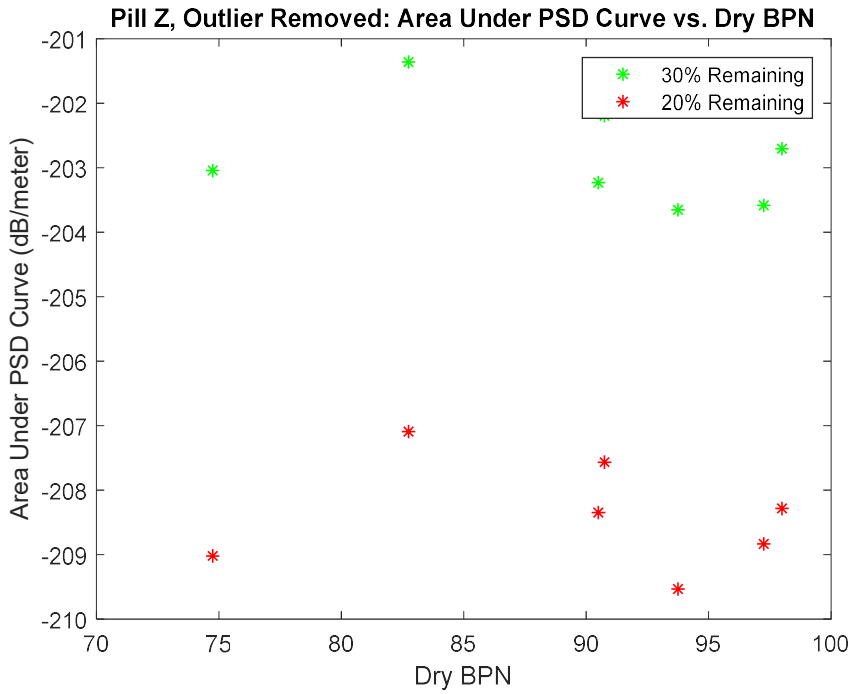

Figure 52: Pill Z Area Under PSD Curve vs. Dry BPN; Data Removed

Figures 53 and 54 show PSD slope vs. Dry BPN. Note that no clear trend can be seen.

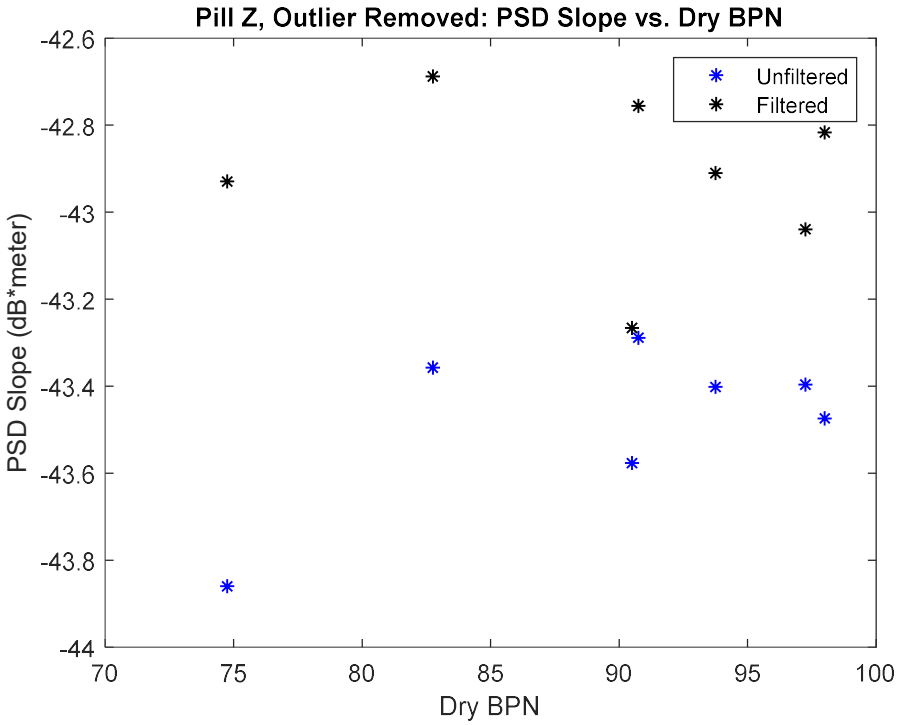

Figure 53: Pill Z PSD Slope vs. Dry BPN; Unfiltered/Filtered

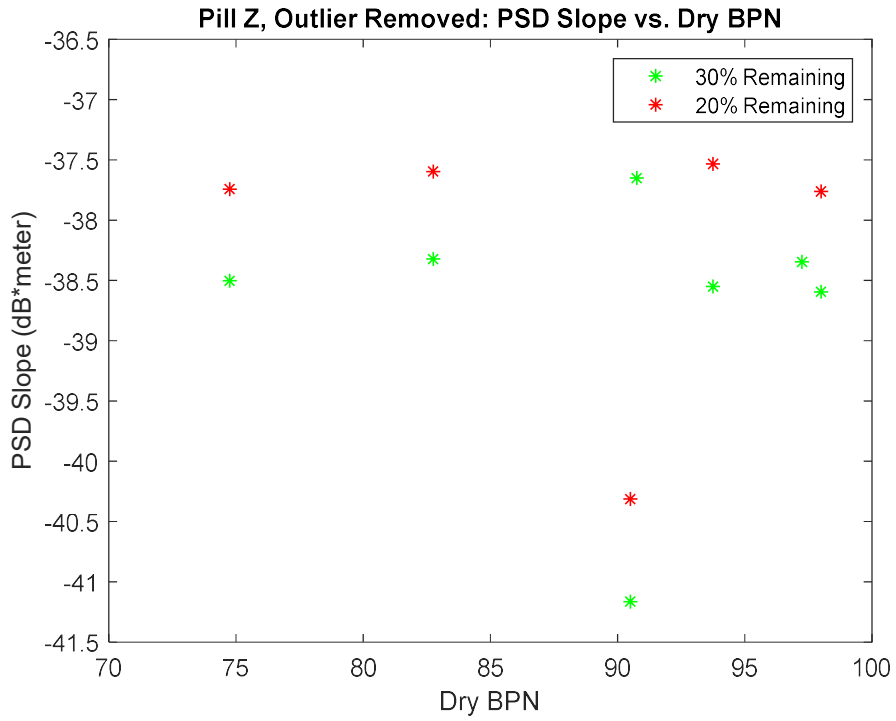

Figure 54: Pill Z PSD Slope vs. Dry BPN; Data Removed

Note that for pill Z no trends can be identified in any of the plots comparing polishing, friction, and PSD metrics with each other.

BPN Variation with Orientation

Through special care detailed earlier in this chapter was taken in order to conduct BPT testing in the same location on the pill between each run, human error is still involved to some degree. In order to assess the severity of the effect on pill orientation on BPN the flip side of pill B from the pilot study, which was unpolished, was examined on the BPT. The pill was struck and then rotated 45 degrees until the original testing site was reached. Again, 4 runs were averaged to obtain the BPN for each orientation. The results for wet and dry conditions can be seen in the figures 55 and 56.

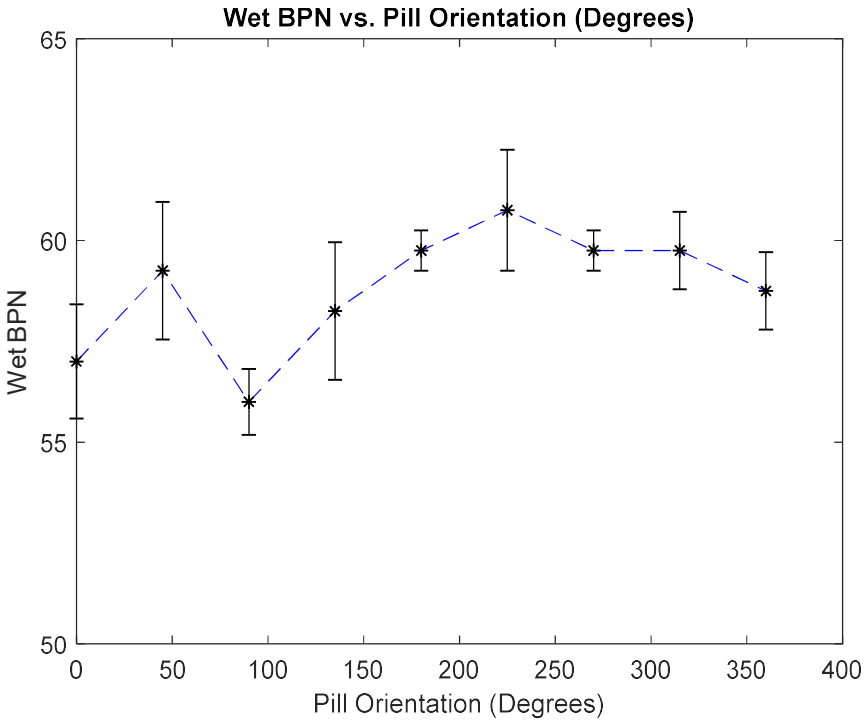

Figure 55: Wet BPN vs. Pill Orientation

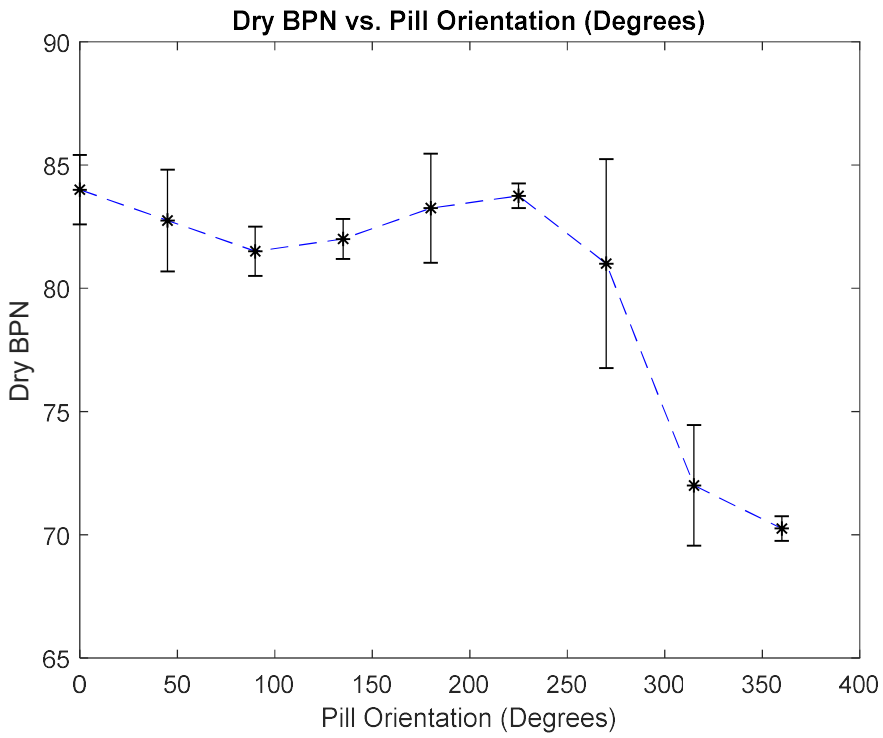

Figure 56: Dry BPN vs. Pill Orientation

A range of about 5 BPN for wet and 15 BPN for dry conditions was discovered to exist over the measurements taken. Most interesting are the data points at the same location (zero degrees and 360 degrees) which theoretically should have identical BPN. For wet these points had about a 2 BPN difference whereas for dry they had a difference of about 13 BPN.

Conclusions

Multiple plots of PSD, polishing time, and BPN metrics showed apparent trends for pill Y. However, none of these trends could be reproduced by the results of pill Z.

It was also determined that there is a reasonable amount of variability in the BPT measurements especially related to pill orientation.

The polishing interval of 15 minutes was unable to produce results suitable for drawing a correlation between wear and friction.

Chapter 4: Conclusions

AMES Scanner Capability Study

Conclusions

In both cores studied, the 9500 was able to reproduce and accurately represent the pre-slope regions of the PSD plots. The 9500 was able to reproduce a small portion of the sloped region for core 33 but was not able to represent the slope region for core 16 at all. Due to the variations present in the slope region, the metrics computed from the 9500 PSD plots had significant error compared with those calculated using the 9300's PSD plots.

The 9500 showed some promising capabilities but based upon on the work and findings of this study alone, the 9500 can be neither verified nor rejected as a capable tool.

Future Work

To be able to reach a final conclusion about the aptness of the 9500 more cores should be scanned. A sample of two to three more cores with randomly assorted aggregate and one more irregularly distributed core is suggested. This will give a good sample size for cores similar to core 33 to be able to determine repeatability of the 9500's pre-slope region success and will offer more insight into how much of the slope region can be accurately represented by the 9500. Scanning another irregular core like core 16 will tell if the results of core 16 were anomalies based on the core or if irregular distributions in general are a problem area for the 9500.

To further test the capability, the preserved slope region on the core 33 sample and other future samples should be extrapolated over the whole slope region. With the bad slope data erased and this preserved slope projected over the region, the metrics should be recalculated and checked to

see how they match with the metrics based on the 9300. It is possible that an extra bit of post-processing on 9500 scans such as this will cover the disparity in resolution between the two machines allowing the team to take advantage of the 9500's vastly superior scan time.

If it is determined that the 9500 is adequate, then scanning a large section of road should be a next step. Scanning a large area such as a 10 ft. by 10 ft. section of a corner on a road or track will give insight into the variability of road surface and the effects of high stress on the road surface. This will remedy the suspicion that the using the scan areas in this study are insufficient to characterize a road surface wholly.

Another next step is scanning the same core multiple times in different orientations and slight height above surface variations. Studying the error between measurements of the same surface with different orientation will give insight into the general effectiveness of all three AMES scanners discussed.

Polishing Study

Conclusions

The comparison results for pill Y showed some promising and clear trends. It was noted that for a few of these trends the 30% and 20% data remaining cases were not able to replicate the trends seen in the unfiltered and filtered data. This could be indication that the data removal percentages are not accurate. Pill Z was not able to show repeatability of any of the trends seen in the pill Y data. Wet BPN results exhibited the expected trend of decreasing friction with polishing time. Dry BPN however, did not show expected trends. Dry BPN also showed a significant amount of error during orientation testing. The combination of these two facts could mean that the BPT is

sensitive to too many variables in dry conditions to be a useful tool for the polishing study at this time.

Future Work

Since friction performance tends to, depending on surface composition, either deplete or improve over time in real world application we believe that there is a meaningful link between state of wear and available friction. This means this study is worth continuing. It is unclear if the 15-minute interval was successful. There are three currently possible sources of error in this study which represent a high threat to the success of the study. These are: inconsistencies between pills, BPT not being able to repeatably measure friction in dry conditions, and uncertainty about the appropriateness of the 15-minute interval. In order to eliminate polishing time as a possible source of error more polishing frequencies need to be examined. More frequent and less frequent intervals should both be conducted, and all intervals should be compared to determine if interval time is a significant source of error. The results can then be contrasted to search for insight into polishing time. Further work will also need to be done to understand the erratic results of dry BPT and if the variability of pill construction causes high error between samples.

FEM Tire Model

Future Work

Since the FEM model is only 2D it does not account for the areas of tire tread where contact patch area is lost. Adapting the model to a 3D tire would more accurately account for the percentage of a scan that the tire will actually use. This is important because removing the correct percent of data from a scan leads to optimization in processing time while preserving the relevant surface roughness data. .

Final Thoughts

This thesis set out to examine the relationship between wear and friction by using The Polisher to simulate accelerated wear due to travel on two road samples. It was learned form this study that British Pendulum tester results for dry BPN are sporadic and susceptible to too many unknown variables to be a useful metric at this time. Some promising trends were noticed for one sample, pill Y, though these trends were not found to be repeatable on pill Z. To inspect some sources of error in the study, a separate sample was tested at different orientations on the BPT. This test further showed that dry BPN is not currently a useful measurement due to the high variation of results based solely on orientation. Wet BPN was also found to have some error associated with orientation but the magnitude was not very large. Other sources of error could be pill construction and polishing interval. The polishing Study was unable to draw a correlation between the state of wear of a surface represented by surface characteristics of PSD plots and the available friction of a surface as measured by a British Pendulum Tester.

References

[1] Bhushan, B., “Introduction to Tribology, Second Edition” (John Wiley & Sons, Ltd, 2013), Chapter 2, ISBN: 978-1-119-94453-9.

[2] Walton, Ryan J. “Characterization of Road Surfaces Using High Resolution 3D Surface Scans to Develop Parameters for Predicting Tire-Surface Friction.” The Ohio State University, 2018.

[3] Sekar, Rubanraj. Road Surface Characterization Post-Processing Report. Unpublished Internal Report

[4] Staschiak, Joey. Weekly Reports. Unpublished Internal Report

[5] “The Closest Race Finishes In NASCAR History.” SportsBreak, www.sportsbreak.com/racing/the-15-closest-race-finishes-in-nascar-history/.

[6] “Chapter 10 - Tires.” Fundamentals of Vehicle Dynamics, by Thomas D. Gillespie, SAE International, 1992, pp. 340–342.

[7] “Home > Slip Testing > Wet Pendulum.” Slip Check, www.floorsliptest.com.au/wet-pendulum/.